SUPPLEMENTAL MATERIAL

EXPANDED METHODS

Data availability

The authors declare that the majority of supporting data are presented within this article and the online Supplement. Data not directly presented are available from the corresponding author upon reasonable request. Raw single-cell data have been deposited in the ArrayExpress database at EMBL-EBI (www.ebi.ac.uk/arrayexpress) under accession number E-MTAB-9703).

Generation/origin of mouse strains

Animal experiments were approved by the KU Leuven Ethics Committee on Animal Use (P003/2012 and P215/2015). Three transgenic mouse lines were used: ubiquitous constitutive *Prdm16* knock-out mice (*Prdm16*$^{Gt(OST67423)Lex}$; refered to as '*Prdm16*$^{+/-}$') were purchased from Mutant Mouse Resource & Research Centers (MMRRC) and backcrossed for 9 generations on a C57Bl/6 background;[13] endothelial cell (EC)-specific *Prdm16* knock-out mice (*Cdh5-Cre*^{ERT2}*;Prdm16*$^{fl/fl}$; refered to as '*EC-Prdm16*$^{-/-}$') were generated by inter-crossing the tamoxifen-inducible *Cdh5-Cre*^{ERT2} driver line (available through R. Adams, Münster, Germany)[18] with *Prdm16*$^{fl/fl}$ mice (available through B. Spiegelman, Boston, USA),[19] both on a C57Bl/6 background; mice with a deficiency for *Prdm16* in smooth muscle cells (SMCs; *Sm22α-Cre;Prdm16*$^{fl/fl}$; refered to as '*SMC-Prdm16*$^{-/-}$') were generated by crossing the constitutively active *Sm22α-Cre* driver line (mixed CD1/C57Bl/6 background; available through J. Herz, Texas, USA)[20] into the *Prdm16*$^{fl/fl}$ strain. Animals were kept under a 12hour/12hour light/dark cycle and allowed access to standard rodent chow and water *ad libitum*.

Adverse events and animal exclusion

During the course of the experiments, 5 animals died (1 *Prdm16*$^{+/-}$, 3 *EC-Prdm16*$^{-/-}$ and 1 *SMC-Prdm16*$^{+/+}$) and 23 animals were excluded (4 *Prdm16*$^{+/+}$, 7 *Prdm16*$^{+/-}$, 6 *EC-Prdm16*$^{+/+}$ and 6 *EC-Prdm16*$^{-/-}$) from outcome analysis due to technical problems (*i.e.*, failed immunostaining, non-responsiveness to one or more vasoactive agents during *ex vivo* vasomotor function testing or loading artifacts during immunoblotting).

Prdm16 expression analysis

To study the expression pattern of Prdm16, two different techniques were used. The first method took advantage of the presence of a gene trap cassette in the *Prdm16* locus encoding

β-galactosidase in *Prdm16*$^{+/-}$ mice.[13] Adult *Prdm16*$^{+/-}$ mice were perfused with 0.2 % adenosine (Sigma-Aldrich, A9251) and fixation solution (PBS containing 0.2 % glutaraldehyde and 2 mmol/L $MgCl_2$) for 5 minutes before dissection of vascular beds and starting the X-gal staining protocol. Briefly, dissected tissues were washed three times with PBS for 10 minutes and incubated overnight at 30°C with staining solution (PBS containing 1 mg/mL X-gal (Life Technologies, 15520-034), 5 mmol/L $K_3Fe(CN)_6$, 5 mmol/L $K_4Fe(CN)_6$ and 2 mmol/L $MgCl_2$). The following day, tissues were washed three times with PBS for 10 minutes and fixed with 4 % paraformaldehyde (PFA) for 2 hours at room temperature. Prior to processing for paraffin embedding, a final PBS washing step was performed. Samples were sectioned and cross-sections were counterstained with nuclear fast red dye. *Prdm16*$^{+/+}$ littermates served as negative controls. While whole-mount stained adult tissues were processed for paraffin embedding and sectioned, whole-mount stained retinas from adult mice were flat-mounted with Prolong™ Gold Antifade reagent (Life Technologies, P36934) before imaging. For the second method, a staining protocol was optimized for immunofluorescence analysis. Briefly, tissues were dissected out, snap-frozen in liquid N_2 and stored at -80°C until cryo-sectioning. Samples were mounted with Tissue-Tek and 7 μm sections were made using a Leica 3050S cryostat. Sections were air-dried and fixed with 4 % PFA for 10 minutes. Next, sections were washed with MilliQ water, washed three times with TNT (TNB + 0.05 % Tween-20) and subsequently permeabilized with PBS containing 0.1 % Triton for 30 minutes. Non-specific protein interactions were prevented by incubating slides with blocking buffer (TNB containing 10 % donkey serum) for 45 minutes. Slides were incubated overnight at 4°C with sheep anti-Prdm16 antibody (R&D Systems, AF6295, 1:100). The next day, slides were washed three times with TNT and incubated with donkey anti-sheep-IgG-Alexa-488 antibody (Jackson Immunoresearch Laboratories, 713-546-147, 1:200) and Cy3-conjugated anti-α-smooth muscle actin (αSMA; Sigma-Aldrich, C6198, 1:1,000) for 2 hours at room temperature. Nuclear staining was obtained by incubating slides with TO-PRO-3 iodide (ThermoFisher Scientific, T3605, 1:1,000) for 15 minutes. Finally, slides were mounted with Prolong™ Gold Antifade. For quantification of the Prdm16 expression signal in ECs or SMCs at different time-points post-ligation, confocal pictures were taken from several collaterals on the ligated (L) and the unligated (UL) side of adductor region cross-sections of *Prdm16*$^{+/+}$ mice. The mean fluorescence intensity signal in ECs and SMCs was measured separately on the intimal layer (defined as the layer within the internal elastic lamina) and the medial layer, respectively, and the L/UL ratio was calculated. Antibodies used for immunostaining were

validated during optimization of the staining procedure during which a negative control condition was included (*i.e.*, an identical staining procedure with exclusion of the primary antibody). In case of staining for Prdm16, the antibody was validated by loss of staining upon *Prdm16* knock-out.

Structural and biomechanical vessel measurements

Adult vessels collected for Prdm16 expression analysis were also used to study structural vascular dimensions of *Prdm16*$^{+/+}$ and *Prdm16*$^{+/-}$ mice. Inner diameter (mm) and SMC cross-sectional area (mm^2) of descending aorta (DA) and femoral arteries (FA) were measured by ImageJ software (version 2.0). Biomechanical measurements were obtained on separate sets of mice by mounting DA segments in a Rodent Oscillatory Tension Set-up to study Arterial Compliance (ROTSAC), as described.[21] In brief, 2 mm aortic segments were collected, cleaned from surrounding tissue and mounted in 8 mL organ baths containing Krebs-Ringer solution (118 mmol/L NaCl; 4.7 mmol/L KCl; 2.5 mmol/L $CaCl_2$; 1.2 mmol/L KH_2PO_4; 1.2 mmol/L $MgSO_4$; 25 mmol/L $NaHCO_3$; 0.025 mmol/L CaEDTA and 11.1 mmol/L glucose) maintained at 37°C and aerated with 95 % O_2 and 5 % CO_2. Segments were exposed to alternating (10 Hz) preloads corresponding to physiological systolic (120 mm Hg) and diastolic (80 mm Hg) blood pressure. Biomechanical parameters of *Prdm16*$^{+/+}$ and *Prdm16*$^{+/-}$ mice were evaluated by calculating compliance (C) and Peterson's Modulus (Ep). The equation for C used was: $C = \frac{\Delta D}{\Delta P}$ with ΔD the difference between inner diameter of the mounted segment under systolic and diastolic pressure and ΔP the difference in systolic and diastolic pressure. In addition, Ep was calculated using following equation: $E_P = \frac{D_0}{C}$ with D_0 the inner diameter at diastolic pressure.

Cell type-specific deletion

EC-specific *Prdm16* deletion was induced by injection of tamoxifen (Sigma-Aldrich, T564) dissolved in sunflower seed oil (Merck, S5007). Long-term EC-specific deletion was obtained by 4 consecutive intra-gastric injections of 50 µL of increasing doses of tamoxifen (1 mg/mL at postnatal day (P)1 to 2.5 mg/mL at P4) in new-born *EC-Prdm16*$^{-/-}$ and *EC-Prdm16*$^{+/+}$ littermates. Short-term EC-specific deletion was induced by intraperitoneal injection of 10-week old *EC-Prdm16*$^{-/-}$ and *EC-Prdm16*$^{+/+}$ littermates with 200 µL tamoxifen (10 mg/mL) for 5 consecutive days, the first injection being performed 14 days prior to induction of hind limb ischemia (HLI). The effectiveness of tamoxifen-induced deletion was ~80 % in both short-term and long-term deletion mice (determined by calculating the percentage of Prdm16$^+$ arterial ECs lining collaterals in the adductor region of tamoxifen-treated mice using our in-house

developed Prdm16 staining protocol; Online Figure I). By combining Prdm16 staining with αSMA staining, Prdm16 deletion in collaterals was shown to be restricted to ECs or SMCs in *EC-Prdm16*$^{-/-}$ and *SMC-Prdm16*$^{-/-}$ mice, respectively (Online Figure I).

Blood pressure measurements

Blood pressure measurements were performed on a CODA system (Kent Scientific) via non-invasive tail cuff measurements. Mice were trained for three days prior to measurements to adapt to recording conditions. Briefly, mice were placed in a constrainer and placed on a heating pad to maintain body temperature. To register blood volume and pressure changes, two cuffs were placed around the tail of the animal. First, animals were allowed to acclimate to the conditions via ten acclimation recording cycles. Next, two cycles of 5 measurements were performed to calculate systolic and diastolic blood pressure. Measurements were averaged to obtain final values.

HLI induction

HLI studies were performed in 8- to 12-week old adult *Prdm16*$^{+/-}$, *EC-Prdm16*$^{-/-}$, *SMC-Prdm16*$^{-/-}$ male and female mice and their corresponding wild-type (WT) littermates. Mice were anesthetized via an intraperitoneal injection of a mixture of xylazine (1.6 mg/mL) and ketamine (20 mg/mL). Body temperature was maintained by placing animals on a 37°C heating pad. Prior to surgery, fur was removed with depilatory cream and skin was disinfected with 70 % ethanol. The skin was opened at the adductor region with an incision parallel to the direction of the femoral artery. The right femoral artery was ligated by applying titanium hemostatic clips (Vitalitec, W6060-1) proximally and distally to the bifurcation of the *arteria femoralis* with the *arteria epigastrica* and *arteria profundis femoris*, and the segment between the hemostatic clips was cut, as described.[7] The incision was closed with surgical stitches using a surgical Ethilon 3.0 thread (Ethicon, EW320) and disinfected with iodine. The left leg was not operated and served as an internal control. Reperfusion recovery was monitored by repeated laser doppler imaging (Lisca, PIMII) under 2 % isoflurane-induced sedation and under body temperature-controlled conditions at day (d)0, d3, d7, d10, d14 and d21. At d21, mice were perfused with 0.2 % adenosine to obtain vasodilation and fixated by perfusion with zinc formalin (Sigma-Aldrich, Z2902) for 5 minutes. Adductor and gastrocnemius muscles were dissected-out, post-fixed overnight with zinc formalin fixative and processed for paraffin embedding. In a subset of mice, adductor muscles were dissected-out at d3 post-ligation for inflammatory cell recruitment analysis. In another subset of mice, adductor and gastrocnemius

regions from the ligated and unligated side at d3 post-ligation were snap-frozen and stored (at -80°C) until further use for extraction of total RNA or protein (see below).

Scoring of necrosis, fibrosis and fibro-adipose tissue

Following femoral artery ligation, necrosis was repeatedly assessed by an in-house developed necrosis score by an observer blinded to the genotype. The first step in the scoring process was to assign 4 levels of necrosis to each of the 5 toes of the limb at the ligated side: 'normal' or 'no necrosis', 'black toe nail', 'necrotic toe' and 'amputated toe' whereby the 'no necrosis' level corresponds to a score of 0, the 'black toe nail' level corresponds to a score of 1, the 'necrotic toe' level corresponds to a score of 2 and the 'amputated toe' level corresponds to a score of 3. The second step was then to make for each mouse a total score by adding up the scores for the 5 toes. The scoring was done repeatedly for the same mice at different time points after the ligation. To investigate signs of fibrosis in the gastrocnemius muscle at an early stage, *i.e.*, d3 post-ligation, gene expression was determined by qRT-PCR (see below) and to evaluate fibrosis in d21 post-ligation gastrocnemius muscles, cross-sections were deparaffinated, rehydrated and stained with Sirius red dye solution. The Sirius red dye stains matrix fibers such as collagen both in their mature and immature form. The fibrosis score was determined by measuring the relative area of muscle fibrosis on microscopic images with ImageJ software. Fibro-adipose tissue (defined according to Meisner *et al.*)[22] was quantified on Sirius red-stained sections at d21 post-ligation. Morphometric analysis was performed by an investigator unaware of the mouse genotype. Representative images for each condition represent the group average determined by the corresponding quantification.

Analysis of collateral remodeling and capillary density

Collateral remodeling in the adductor region was first evaluated by studying the recruitment of inflammatory cells around the growing collaterals at d3 post-ligation. Cross-sections of adductor muscle were deparaffinated and rehydrated. Next, antigen retrieval was performed by boiling slides for 20 minutes in target retrieval solution (Dako, s1699) followed by 20 minutes cooldown. Slides were washed three times with TBS for 5 minutes and incubated with methanol containing 0.3 % H_2O_2 to inactivate endogenous peroxidase activity. After three TBS washing steps, slides were blocked with TNB containing 20 % serum for 45 minutes. Next, slides were incubated with an anti-Cd45 antibody (Beckton Dickinson, BD553081, 1:100) or anti-Cd68 antibody (Abcam125212; 1:100) overnight. Prior to secondary antibody incubation, slides were washed three times with TNT. A biotinylated donkey anti-rabbit IgG secondary antibody (Santa Cruz, sc-2089; 1:300) dissolved in TNB containing 10 % serum was applied

on the slides for 45 minutes. Next, a TSA biotin detection kit (PerkinElmer, NEL700A001KT) was used to amplify the fluorescent signal as described by the provider. Briefly, slides were incubated with Streptavidin-HRP (1:100) dissolved in TNB for 30 minutes, washed three times with TNT and incubated for 8 minutes with A-diluent containing Cy3 (1:50). Following amplification, slides were washed with TNT and incubated with FITC-conjugated mouse-anti-αSMA (Sigma-Aldrich, F3777, 1:200) for 2 hours. Prior to mounting with Prolong™ Gold Antifade containing DAPI (Life Technologies, P36931), final TNT washing steps were performed. The number of $Cd45^+$ or $Cd68^+$ cells in close proximity of 6 expanding collaterals were counted on 6 different cross-sections and results were averaged to obtain the amount of $Cd45^+$ or $Cd68^+$ cells per mouse.

To study the remodeled collateral network at d21 post-ligation, collaterals were identified by co-staining transversal adductor region cross-sections for Cd31 and αSMA. After deparaffination and rehydration, cross-sections were incubated with methanol containing 0.3 % H_2O_2 for 20 minutes. Prior to overnight incubation with primary antibodies (TNB containing anti-Cd31 (Beckton Dickinson, BD557355, 1:500) and anti-αSMA-Cy3 (Sigma-Aldrich, C6198, 1:200) slides were incubated with TNB for 45 minutes. The next day, slides were washed with TNT and incubated with a biotinylated secondary antibody (TNB containing 10 % serum and rabbit anti-rat IgG-biotin, Invitrogen, A18919, 1:500). As described above, the signal was amplified and visualized by using a TSA biotin detection kit (PerkinElmer, NEL700A001KT). Next, slides were washed and mounted with Prolong™ Gold Antifade mountant containing DAPI. Remodeled collaterals were identified as described previously.[6] ImageJ software was used to measure the luminal diameter and SMC cross-sectional area of the identified collaterals. The unligated side served as an internal control to evaluate the collateral remodeling process. To determine capillary density in the gastrocnemius muscle, an identical Cd31/αSMA staining protocol was used. $Cd31^+$ structures were counted and normalized for muscle area. In total, 6 pictures were analyzed for each gastrocnemius muscle. Antibodies used for immunostaining were validated during optimization of the staining procedure during which a negative control condition was included (*i.e.*, an identical staining procedure with exclusion of the primary antibody). All morphometric analysis was performed by an investigator unaware of the mouse genotype. Representative images for each condition represent the group average determined by the corresponding quantification.

Nano-computed tomography (Nano-CT)

To obtain an integrated view on the vascular architecture of the adductor region, *Prdm16*$^{+/-}$ mice (*n*=4) and *Prdm16*$^{+/+}$ littermates (*n*=3) were subjected to femoral artery ligation and 7 days later anesthetized with ketamine/xylazine and perfused with 0.2 % adenosine for vasodilation, then with 4 % paraformaldehyde for fixation and then with saline to wash out the fixative, followed by a preheated solution of 30 % barium sulphate (Micropaque, Guerbet) suspended in a 2 % gelatin solution. To solidify the gelatin and fix the contrast agent in the vessels, mice were stored on ice at 4°C overnight. The next day, hind limbs were dissected out and stored in PBS. Subsequently, hind limbs were scanned with a Phoenix Nanotom M (Waygate Technologies). Limbs were scanned at 6 µm voxel size. The source, equipped with a tungsten target, was operated at 50 kV and 200 µA and a 0.5 mm Aluminium filter was applied. For each limb, 1,000 frames were acquired over 360° using the fast scan mode with an exposure time of 500 milliseconds (frame averaging = 1 and image skip = 0), resulting in a scanning time of 8 minutes and 20 seconds per sample. Scan optimization (projection filter, inline volume filter, and beam hardening correction) was applied during three-dimensional reconstruction (Datos/x, Waygate Technologies). Images were analyzed using DataViewer (Bruker Micro-CT, Kontich, Belgium) and Matlab (Mathworks, Natick, US).

Organ bath and wire myograph measurements

DA and FA segments (1-2 mm long) of adult *Prdm16*$^{+/-}$ or long-term *EC-Prdm16*$^{-/-}$ mice and their corresponding WT littermates were dissected-out, cleaned from adherent tissue and mounted between two parallel wire hooks in a 10 mL organ bath or on a 40 µm wire myograph (DMT, 610M), respectively, as described.[23,24] DA segments were subjected to 20 mN preload and FA segments were gradually stretched until wall stress reached the physiological level of 100 mm Hg. Transducers were set at zero to measure active contractions and relaxations. Administration of increasing concentrations of phenylephrine (PE; $3x10^{-9}$ mol/L to $3x10^{-5}$ mol/L) was used to induce vascular contraction while increasing concentrations of acetylcholine (ACh; $1x10^{-9}$ mol/L to $1x10^{-5}$ mol/L) and diethylamine NONOate (DEANO; $3x10^{-10}$ mol/L to $1x10^{-6}$ mol/L; preceded by L-NAME treatment to block endogenous EC-derived nitric oxide production) were used to study EC-dependent and EC-independent vascular relaxation, respectively. To study the effect of HLI on vasomotor function, right femoral segments downstream of the ligation site of *Prdm16*$^{+/-}$ or long-term *EC-Prdm16*$^{-/-}$ mice and their corresponding WT littermates were isolated and mounted in an organ bath of a myograph 3d after the induction of HLI. Corresponding FA segments of the unligated left side

served as an internal control. For *EC-Prdm16*$^{-/-}$ and *EC-Prdm16*$^{+/+}$ littermates, vasomotor function of the DA was also recorded from the same mice.

RNA/protein extraction, quantitative (q) real-time (RT)-PCR and Western blot

For RNA, freshly isolated adductor or gastrocnemius regions were collected from a separate set of *EC-Prdm16*$^{-/-}$ or *EC-Prdm16*$^{+/+}$ littermates. Tissues were crushed on dry ice and suspended in TRIzol. Protein was extracted in radio-immunoprecipitation assay (RIPA) buffer (Sigma, R0278), supplemented with protease and phosphatase inhibitor cocktail (Thermoscientific, #78440, 1:100). RNA was reverse transcribed using Superscript III Reverse Transcriptase (Invitrogen) and for qRT-PCR analysis cDNA was amplified in the presence of SYBR Green dye (Applied Biosystems) using the primer sets listed in Online Table II on a Quantstudio3 (Applied Biosystems), using hypoxanthine-phosphoribosyl-transferase-1 (*Hprt1*) as house-keeping gene. Thermocycle conditions used for qRT-PCR were: hold (50°C, 2 minutes); hold (95°C, 10 minutes); 40 cycles of amplification (95°C, 0:15 minutes / 60°C, 1 minute). Each run was complemented with a melting curve analysis: step 1: 95°C, 0:15 minutes; step 2: 60°C 1 minute; step 3 (dissociation) 95°C, 0:15 minutes. Temperature increment during dissociation was 0.1°C per second. For Western blotting, protein concentrations were measured using the bicinchoninic acid protein assay kit (Thermoscientific, #23225), 40 μg of protein was mixed with reducing reagent (Life Technologies, NP009) and lithium dodecyl sulfate sample buffer (Life Technologies, NP007), loaded on the gel and run at 200 V. Proteins were blotted on a nitrocellulose membrane during 90 minutes at 80 V. For detection of endothelial nitric oxide synthase (eNOS) protein, membranes were incubated with anti-eNOS (BD Biosciences, BD610297; 1:2,000) and donkey anti-mouse IgG-HRP (Santa Cruz, sc-2314; 1:2,000). Bound antibodies were detected using SuperSignal West Femto Maximum Sensitivity substrate (Thermoscientific) on a Bio-Rad ChemiDoc XRS+ molecular imager equipped with Image Lab software (Bio-Rad Laboratories). Bands were quantified using NIH Image software, with Ponceau red staining as loading control.

Single-cell RNA sequencing (scRNAseq)

Cell preparation, library preparation and sequencing. *EC-Prdm16*$^{-/-}$ or *EC-Prdm16*$^{+/+}$ littermates (*n*=4 each) were treated with tamoxifen at P1 to P4 and were subjected to right femoral artery ligation in adult stage. Three days later, femoral artery segments downstream of the ligation and the corresponding segment on the unligated side were efficiently dissected-out and collected on ice. To obtain sufficient amounts of cells for sequencing, for each genotype and for each side, the segments from all 4 mice were pooled. Pooled FA segments were

mechanically dissociated using a scalpel, and subsequently enzymatically dissociated in digestion medium (2 mg/mL Collagenase P (Sigma Aldrich) and 0.2 mg/ml DNAse I (Roche) in DMEM (Thermofisher scientific)). Red blood cells were removed from the cell suspension using red blood cell lysis buffer (Roche), and cells were filtered using a 40 µm Flowmi tipstrainer (VWR). Next, the isolated cells were immediately counted by a Luna-FL Dual Fluorescence Cell Counter (Logos Biosystems) and 4 mouse single-cell libraries (*EC-Prdm16*$^{-/-}$ ligated and unligated, *EC-Prdm16*$^{+/+}$ ligated and unligated) were prepared with the Chromium Single Cell 3' V2 Chemistry Library Kit, Gel Bead & Multiplex Kit and Chip Kit from 10X Genomics. The barcoded libraries were sequenced on an Illumina Nextseq and NovaSeq6000 in 25-8-98 paired-end configuration up to a saturation over 60 %.

scRNA data analysis. Raw sequencing reads were demultiplexed, mapped to the mouse reference genome (build mm10) and gene-expression matrices were generated using CellRanger (version 2).[27] On average 84,180,999 [67,924,026 - 94,406,237] reads were mapped per sample. The gene-expression matrices were further analyzed in Seurat 2.0 installed on R version 3.6.0 "Planting of a Tree", unless otherwise stated. Single cells with less than 200 genes or 400 unique molecular identifiers (UMIs) were discarded as well as cells with more than 20 % of mitochondrial (mt)RNA (Online Figure II), resulting in 6,758 single cells across the 4 samples. After normalization, the 2,000 most variable genes were selected and regression was performed on the number of UMIs and the percentage of mtRNA. Next, principal components were constructed and Harmony software[26] was used to reduce batch effects. Clustering was performed at a resolution of 1.0 and a dimensionality reduction was done by Uniform Manifold Approximation and Projection (UMAP) and resulted in 15 clusters. Fourteen clusters were annotated to cell types based on established marker genes and one low-quality cluster was discarded, resulting in 6,392 single cells across the 4 samples (Online Figure II). A comparative quantitative analysis of the *Cd45*$^{+}$ (*Ptprc*$^{+}$) clusters was performed between the 4 sample types. In addition, a two-step differential expression analysis with the MAST algorithm[25] was performed on the expression data related to the arterial EC cluster. The obtained *P*-values were adjusted for multiple testing based on Bonferroni correction using all genes in the dataset. In a first step, we determined for each genotype the genes that were significantly altered by the ligation procedure by comparing the ligated with the unligated side. To obtain differentially expressed gene (DEG) shortlists, raw DEG lists were filtered by leaving out the non-annotated genes and by only retaining those for which (***i***) the adjusted *P*-value was < 0.05; (***ii***) the log fold-change ligated *versus* unligated was > 0.25 (upregulated

genes) or < -0.25 (downregulated genes); (***iii***) the difference in percentage of cells expressing the gene ('pct') in ligated *versus* unligated was > 0.1 (corresponding to > 10 %; upregulated genes) or < -0.1 (downregulated genes). In the second step, we conducted an overlap analysis to determine which genes emerging from step 1 were commonly regulated in both genotypes (which we designated as 'type A' genes) and those emerging from step 1 that were uniquely changed within each genotype (which we designated as 'type B' genes).

Functional annotation analysis. To identify *Prdm16* genotype-dependent cellular functions and pathways, type B genes were analyzed by using a combination of two functional annotation software packages, *i.e.*, Database for Annotation, Visualization and Integrated Discovery (DAVID) functional annotation software (https://david.ncifcrf.gov/summary.jsp) and Gene Set Enrichment Analysis (GSEA) (http://software.broadinstitute.org/gsea/msigdb/genesets.jsp), thereby using the Kyoto Encyclopedia of Genes and Genomes (KEGG) and the Gene Ontology-Molecular Functions (GO-MF) as read-outs.

Lentiviral transduction and Ca^{2+} measurements

A lentivirus overexpressing full-length mouse Prdm16 (Thermo Scientific Molecular Biology; clone ID 6409778) was generated, as described.[9] Human umbilical vein ECs (HUVECs) were generated in house after obtaining informed consent from the donors and were used between passage 3 and 7).[9] Cells were seeded at 125 cells per mm^2 the day prior to transduction and exposed to lentiviral particles with an intermediate media change after two days. After 6 days, cells were harvested by trypsinization and expanded. As a reference control, HUVECs were transduced with a control lentivirus expressing Cherry fluorescent protein. For Ca^{2+} measurements, 50,000 cells were seeded in a gelatin-coated well of a 96-well plate (Greiner Bio-One; 655090) 24 hours prior to Ca^{2+} measurements. Cells were loaded with Fura-2AM (ThermoFisher Scientific; F1221; 1.25 µmol/L) in modified Krebs buffer (135 mmol/L NaCl, 6.2 mmol/l KCl, 1.2 mmol/L $MgCl_2$, 12 mmol/L HEPES, pH 7.3, 11.5 mmol/L glucose and 2 mmol/L $CaCl_2$) for 30 minutes at room temperature. Cells were washed twice with modified Krebs buffer and incubated for 30 minutes at room temperature to allow de-esterification to take place. The total cellular Ca^{2+} content was measured by applying 5 µmol/L ionomycin (Alomone Labs; I-700) to the cells upon chelation of extracellular Ca^{2+} with 3 mmol/L ethylene glycol-bis(β-aminoethyl ether)-N,N,N′,N′-tetraacetic acid (EGTA; Sigma-Aldrich; E3889). The content of endoplasmic reticulum (ER) Ca^{2+} stores was studied using the same conditions but utilizing 2 µmol/L thapsigargin (Alomone Labs; T-650) as stimulus. Store-operated Ca^{2+} entry (SOCE) was studied by treating cells with 2 µmol/L thapsigargin upon chelation of

extracellular Ca^{2+} with 3 mmol/L EGTA to empty the content of the ER Ca^{2+} stores and after 10 minutes cells were exposed to 60 mmol/L $CaCl_2$ to obtain a rapid Ca^{2+} influx in the cells. Ca^{2+} measurements were performed using a Flexstation 3 microplate reader (Molecular Devices). Ca^{2+} measurements were performed on 8 or 12 biological replicates. Biological replicates were represented by 4 different passages of 2 (in case of n=8) or 3 (in case of n=12) different HUVEC clones. Measurements for each passage were done independently on a different day. For each individual Ca^{2+} measurement, cells were plated in duplicate to include two technical replicates. Data were acquired and analyzed using Softmax Pro software (Molecular Devices). Area under the curve values and maximum peak values were calculated using Graphpad Prism7.0 software and compared between experimental conditions.

Statistics

Continuous data are presented as mean ± standard error of the mean (SEM). Continuous data sets were analyzed using Graphpad Prism 7.0, 8.4.3 or 9.0.1, ordinal datasets were analyzed in R (version 4.0.3; package clmm2). Normality of the continuous datasets was evaluated by the Kolmogorov-Smirnov test (if $5 \leq n < 8$) or by D'Agostino & Pearson test (if $n \geq 8$). In case all groups in an experiment had normal distribution, parametric tests were used. In case not all groups in an experiment had normal distribution or normality could not be estimated by the abovementioned tests ($n < 5$), non-parametric tests were used. In case of a repeated measurements ANOVA models, only random effects and residuals were assumed to have a normal distribution. Detailed information related to data distribution and statistical analysis is provided in Online Table III. Briefly, baseline vascular parameters, fibrosis/fibro-adipose tissue measurements, recombination efficiency data, *in vivo* qRT-PCR data and vascular volume measurements were analyzed with a two-sided unpaired Student's *t*-test (or Mann-Whitney test if appropriate; Figure 2*B-I*; Figure 3*D*,*H*,*L*,*P*; Figure 7*D*,*E*; Online Figure IV; Online Figure V,*E*,*J*,*O*,*T*; Online Figure VIII,*B*; and Online Figure IX,*B*). Paired Student's *t*-test was used to analyze the results of *in vitro* Ca^{2+} experiments (Figure 7A-C). Vascular remodeling parameters upon HLI were analyzed using two-way ANOVA with Bonferroni *post-hoc* test (Figure 4*B,C,E,F,H,I,K,L*; Online Figure VII,*F*). Organ bath experiments and laser doppler measurements were evaluated with repeated measures ANOVA and Bonferroni *post-hoc* test (Figure 2*K-O*; Figure 3*B*,*F*,*J*,*N*; Figure 5*B,C,E,F,H,I*; Online Figure IX,*D*,*F*). Sigmoidal dose-response equations with variable slope were used to fit concentration-response curves in the organ bath experiments. Necrosis score data were analyzed by a cumulative link mixed model for ordinal data including time, group and interaction effects (Figure 3*C*,*G*,*K*,*O*).

Data were considered significant if $P<0.05$ (either adjusted or not adjusted for multiple comparison, as indicated in Online Table III). Statistical analysis of the scRNAseq data was performed with the MAST algorithm implemented in Seurat. No experiment-wide multiple test correction was applied as the study was mostly exploratory in nature.

SUPPLEMENTAL FIGURES AND FIGURE LEGENDS

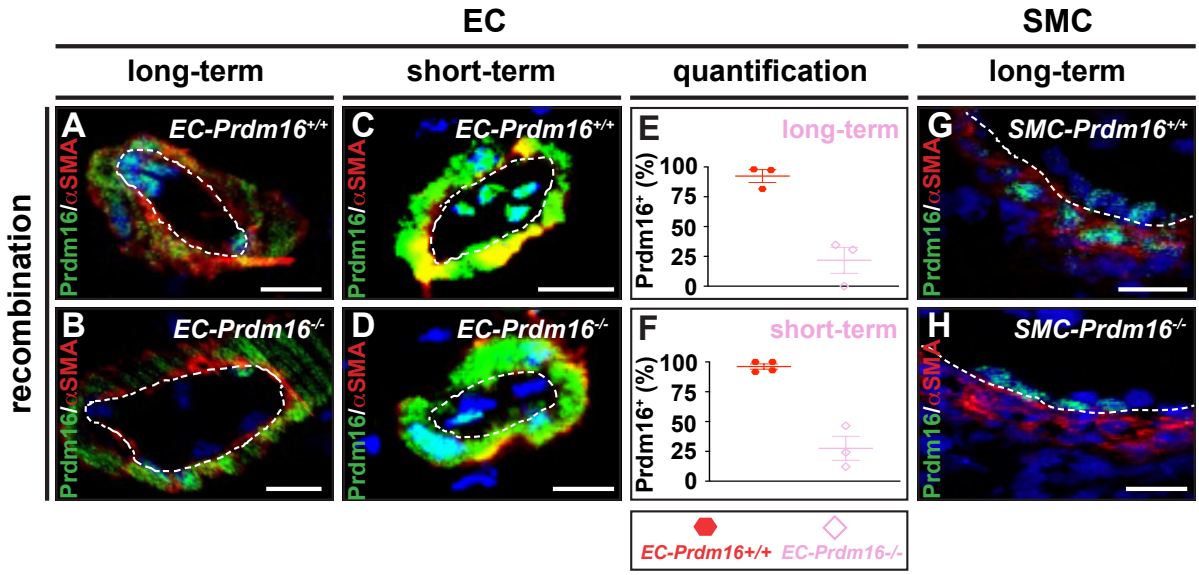

Online Figure I. ***Specificity and efficiency of cell type-specific*** **Prdm16** ***deletion.*** **(A-F)** Cross-sections of collaterals of the adductor region, stained for Prdm16 (green) and αSMA (red) of long-term deleted 10 week-old *EC-Prdm16*$^{+/+}$ (*A*; *n*=3) *versus EC-Prdm16*$^{-/-}$ (*B*; *n*=3) mice or short-term deleted *EC-Prdm16*$^{+/+}$ (*C*; *n*=4) *versus EC-Prdm16*$^{-/-}$ (*D*; *n*=3) mice and corresponding quantification (long-term: *E*; short-term: *F*). Data represent mean ± SEM (Online Table III). **(G,H)** Cross-sections of collaterals of the adductor region, stained for Prdm16 (green) and αSMA (red) of *SMC-Prdm16*$^{+/+}$ (*G*) and *SMC-Prdm16*$^{-/-}$ (*H*) mice. Border between intima and media is lined by white dashed lines and TO-PRO-3 (blue) was used as nuclear counterstaining in *A-D,G,H*. Representative images for each condition represent the group average determined by the corresponding quantification. Scale bars: 25 μm in *G,H* and 10 μm in *A-D*.

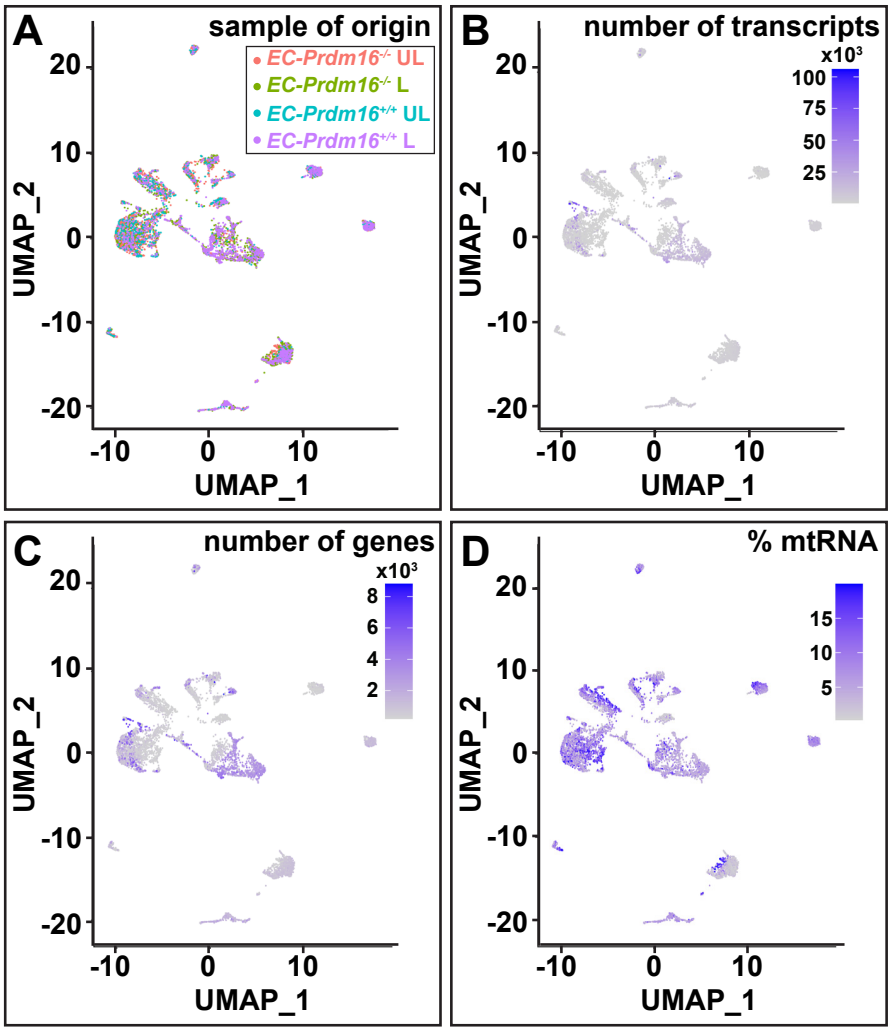

Online Figure II. ***Quality plots of the single-cell RNA sequencing experiment.*** **(A-D)** Uniform Manifold Approximation and Projection (UMAP) analysis of the 6,392 cells profiled here, with each cell color-coded for its sample type of origin (*A*), number of transcripts (unique molecular identifiers; UMIs) detected (*B*), number of genes (*C*) and percentage of mitochondrial (mt)RNA (*D*). Number of cells per sample type: *n*=944 for *EC-Prdm16*$^{+/+}$ UL; *n*=1,726 for *EC-Prdm16*$^{+/+}$ L; *n*=1,975 for *EC-Prdm16*$^{-/-}$ UL; and *n*=1,747 for *EC-Prdm16*$^{-/-}$ L.

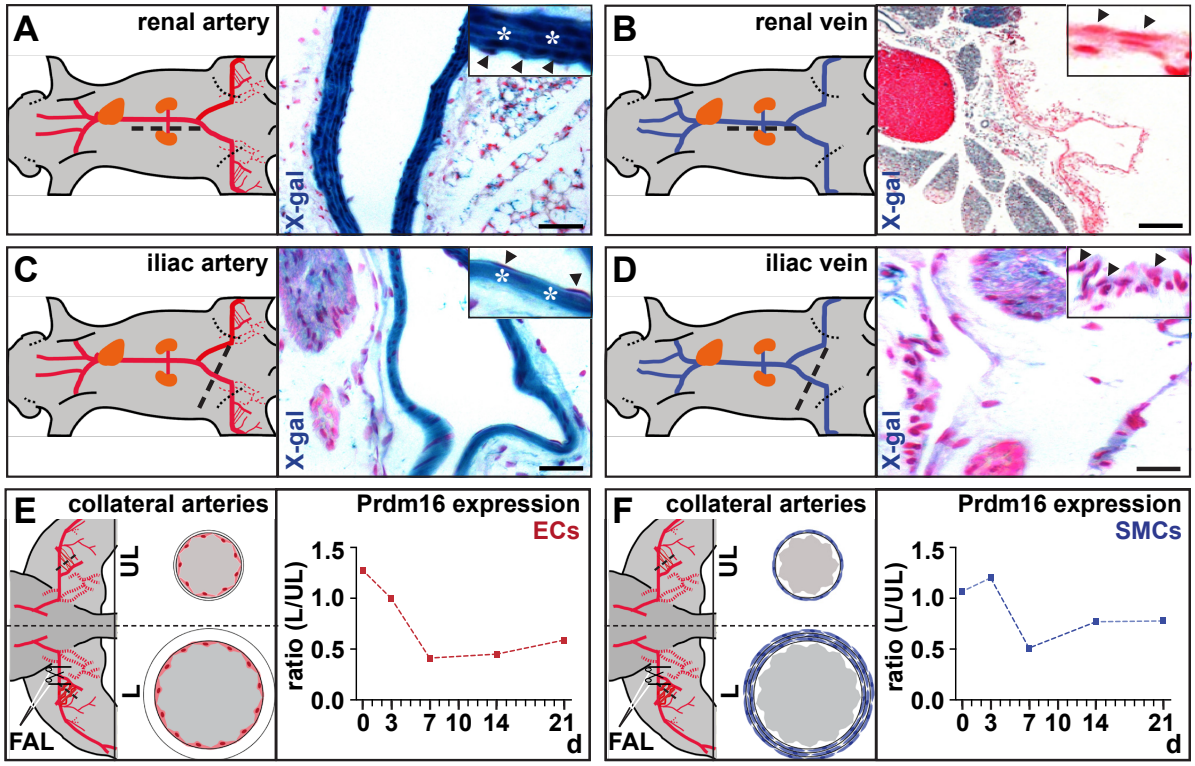

Online Figure III. ***Prdm16 is a universal arterial marker in health and disease.*** **(A-D)** Schematic representation and X-gal staining on cross-sections of different adult *Prdm16*$^{+/-}$ vascular beds. Arteries are shown in (*A,C*) while the venous counterparts are shown in (*B,D*). Shown vascular beds are renal (*A,B*) and iliac vessels (*C,D*). **(E,F)** Schematic representation of a collateral arteriole cross-section (*left*) and quantification of the expression of Prdm16 protein during different days (d) after induction of hind limb ischemia in endothelial cells (ECs in red; *E*) or smooth muscle cells (SMCs in blue; *F*), expressed as the ratio of expression in the ligated (L) over unligated (UL) side. Arrowheads and asterisks in *A-D* indicate ECs and SMCs, respectively. Black dashed lines in *A-D* show location of the cross-sections. Scale bars: 50 µm in *A-D*. FAL: femoral artery ligation.

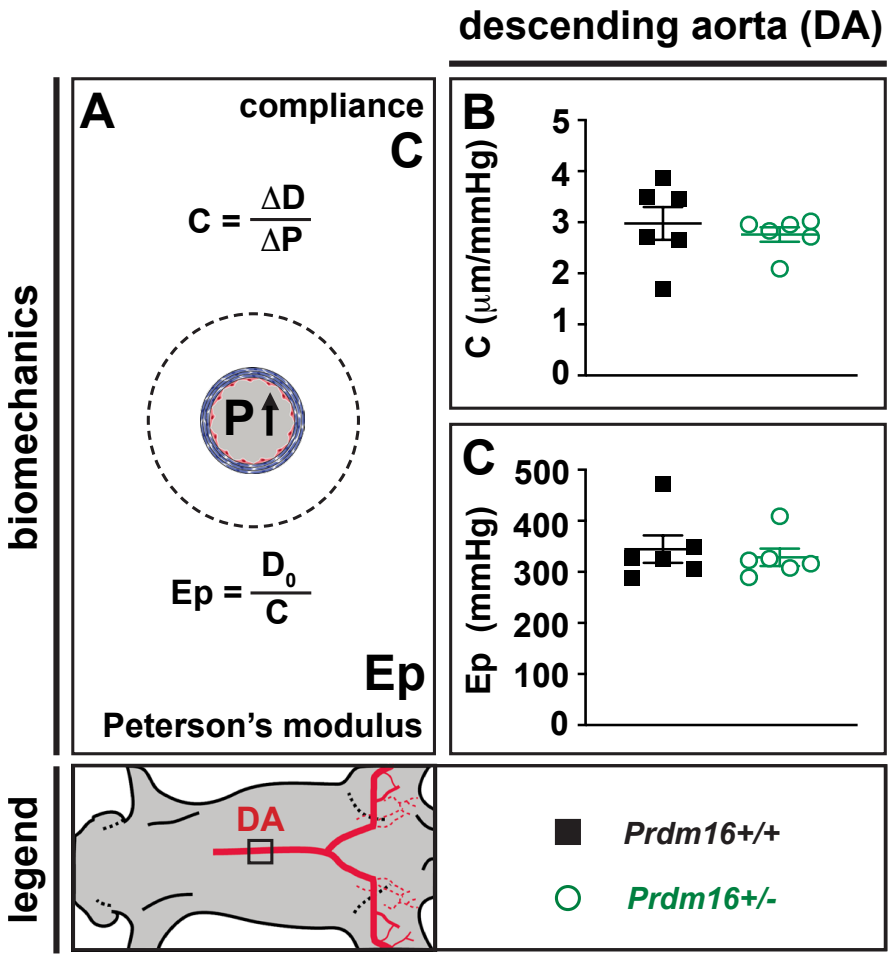

Online Figure IV. Prdm16 ***deficiency does not affect biomechanics of descending aorta segments.*** **(A-C)** Schematic representation (*A*) and quantification of compliance (C) of *Prdm16*$^{+/+}$ (*n*=6) and *Prdm16*$^{+/-}$ (*n*=6) descending aorta (DA) segments (*B*) and quantification of the Peterson's Modulus (E_P) of *Prdm16*$^{+/+}$ (*n*=6) and *Prdm16*$^{+/-}$ (*n*=6) DA segments (*C*). Data represent mean ± SEM (Online Table III).

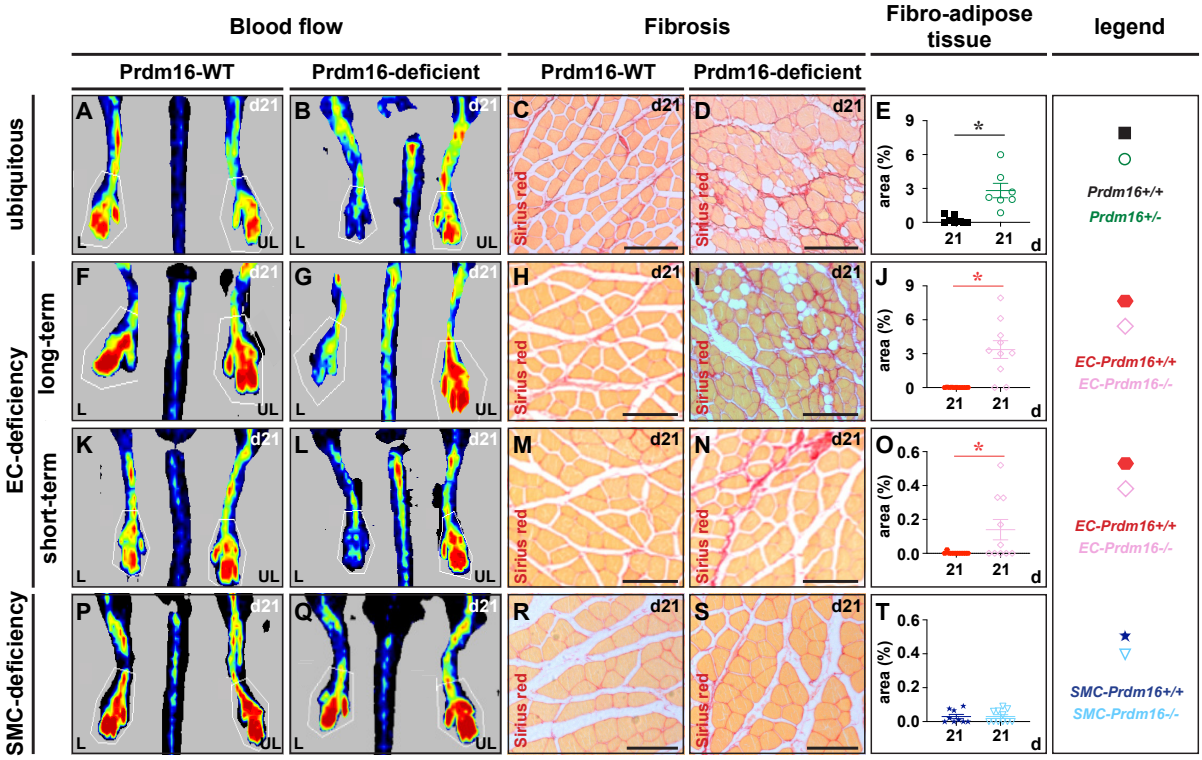

Online Figure V. ***Ubiquitous and EC-specific*** **Prdm16** ***deficiency impairs flow recovery, aggravates fibrosis and increases fibro-adipose tissue formation upon HLI.*** **(A-T)** Representative images of laser doppler recordings (*A,B,F,G,K,L,P,Q*) and Sirius red-stained cross-sections of the gastrocnemius region (*C,D,H,I,M,N,R,S*) and diagrams showing quantification of fibro-adipose tissue (expressed as % *versus* muscle area ± SEM; *E,J,O,T*) at 21 days (d) post-ligation in *Prdm16*$^{+/+}$ (*A,C,E*) or *Prdm16*$^{+/-}$ (*B,D,E*), long-term *EC-Prdm16*$^{+/+}$ (*F,H,J*) or *EC-Prdm16*$^{-/-}$ (*G,I,J*), short-term *EC-Prdm16*$^{+/+}$ (*K,M,O*) or *EC-Prdm16*$^{-/-}$ (*L,N,O*) and *SMC-Prdm16*$^{+/+}$ (*P,R,T*) or *SMC-Prdm16*$^{-/-}$ (*Q,S,T*) mice. (panel *E*: *n*=8 for *Prdm16*$^{+/+}$ and *n*=7 for *Prdm16*$^{+/-}$; panel *J*: *n*=11 for *EC-Prdm16*$^{+/+}$ and *n*=10 for *EC-Prdm16*$^{-/-}$; panel *O*: *n*=11 for *EC-Prdm16*$^{+/+}$ and *n*=10 for *EC-Prdm16*$^{-/-}$; panel *T*: *n*=9 for *SMC-Prdm16*$^{+/+}$ and *n*=11 for *SMC-Prdm16*$^{-/-}$). Data represent mean ± SEM. **P*<0.05 *versus* indicated condition (Online Table III). L: ligated; UL: unligated. Representative images for each condition represent the group average determined by the corresponding quantification. Scale bars: 100 µm.

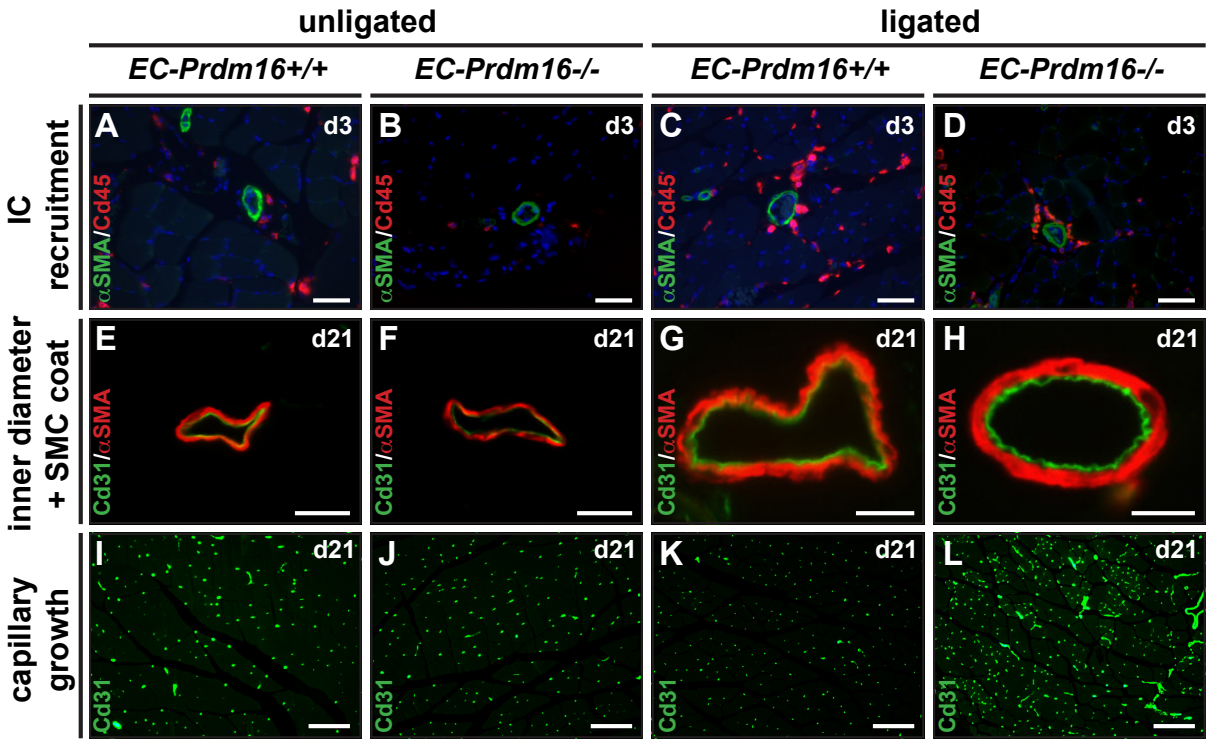

Online Figure VI. ***Long-term*** **Prdm16** ***deficiency in ECs does not affect structural remodeling upon HLI.*** **(A-D)** Representative images of cross-sections of the adductor region stained for αSMA (green) and Cd45 (red) at day (d)3 upon HLI in the unligated side (*A,B*) *versus* ligated side (*C,D*) of long-term *EC-Prdm16*$^{+/+}$ (*A,C*) *versus EC-Prdm16*$^{-/-}$ (*B,D*) mice. DAPI (blue) was used as nuclear counterstaining. IC: inflammatory cell. **(E-H)** Representative images of cross-sections of the adductor region stained for αSMA (red) and Cd31 (green) at d21 upon HLI in the unligated side (*E,F*) *versus* ligated side (*G,H*) of long-term *EC-Prdm16*$^{+/+}$ (*E,G*) *versus EC-Prdm16*$^{-/-}$ (*F,H*) mice. **(I-L)** Representative images of cross-sections of the gastrocnemius region stained for Cd31 (green) at d21 upon HLI in the unligated side (*I,J*) *versus* ligated side (*K,L*) of long-term *EC-Prdm16*$^{+/+}$ (*I,K*) *versus EC-Prdm16*$^{-/-}$ (*J,L*) mice. Representative images for each condition represent the group average determined by the corresponding quantification. Scale bars: 100 μm in *I-L*, 50 μm in *A-D* and 20 μm in *E-H*.

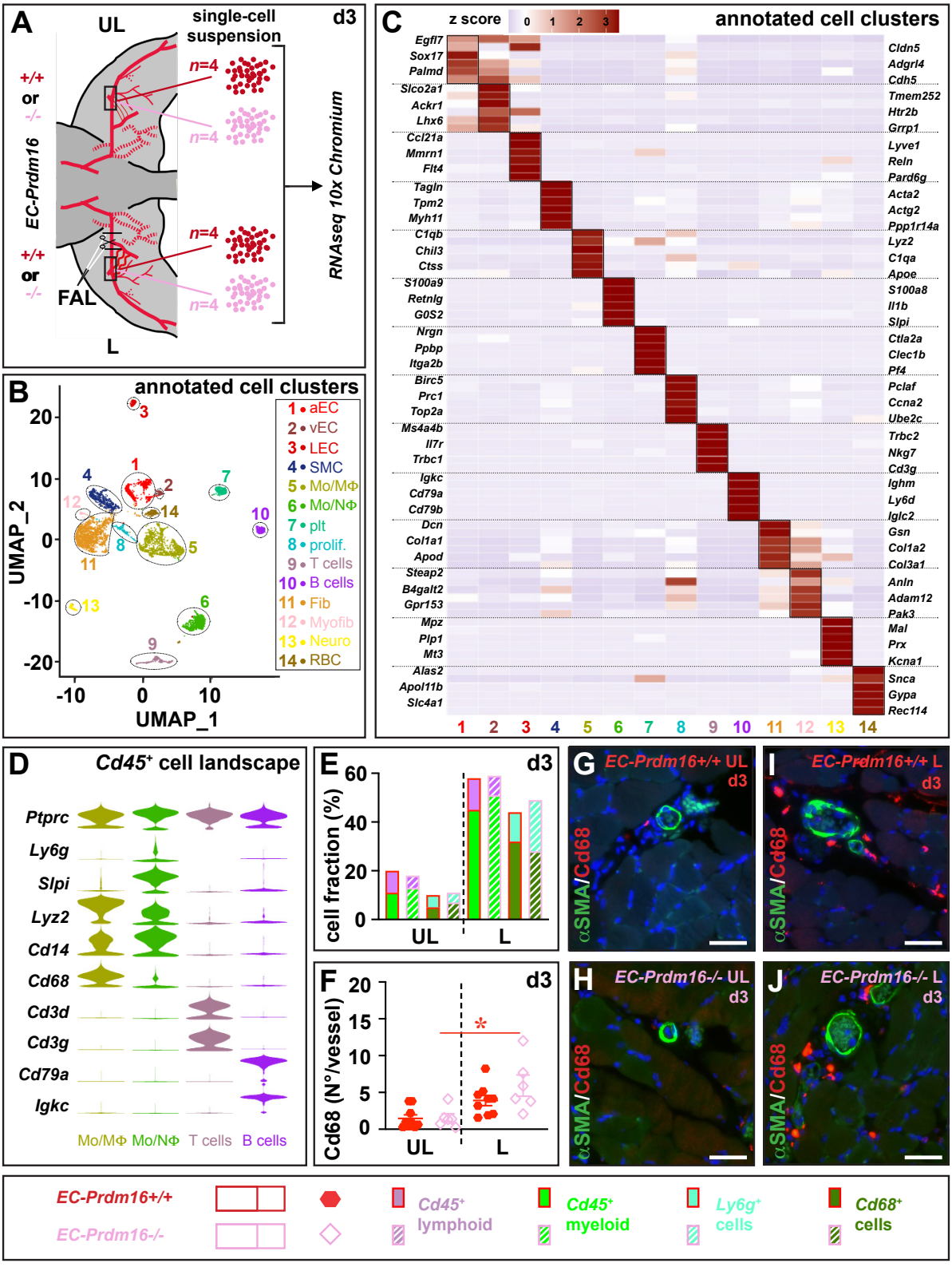

Online Figure VII. ***UMAP analysis of the cellular landscape in the ligated and unligated adductor region of endothelial-specific*** **Prdm16-*deficient mice and their wild-type littermates by single-cell RNA sequencing.*** **(A)** Schematic representation of the study design for the single-cell RNA sequencing experiments at 3 days after femoral artery ligation (FAL).

The region of interest (ROI) from which a single-cell suspension from the ligated (L) or the unligated (UL) side was generated for each of the two genotypes, is indicated by a black box. The ROI material from four animals were pooled to obtain sufficient cells per sample. **(B)** Uniform Manifold Approximation and Projection (UMAP) plot showing 14 numbered annotated cell clusters (aEC: arterial endothelial cell, *n*=588; vEC venous EC, *n*=91; LEC: lymphatic EC, *n*=144; SMC: smooth muscle cell, *n*=605; Mo/MΦ: monocyte/macrophage, *n*=1,225; Mo/NΦ: monocyte/neutrophil, *n*=794; plt: platelet, *n*=302; prolif.: proliferating cell, *n*=158; Fib: fibroblast, *n*=1,561; Myofib: myofibroblast, *n*=61; Neuro: neuron, *n*=111; residual RBC: red blood cell, *n*=207). **(C)** Heat map showing the calculated landmark genes based on which the annotations were performed (6 genes per cluster ranked according to statistical significance). Corresponding color scale is shown on *top*. **(D)** Bean plots showing expression of landmark genes for each of the 4 *Cd45* (*Ptprc*)$^{+}$ annotated clusters. (**E**) Diagram representing the fraction of cells (expressed as % of the total number of sequenced cells) assigned to a *Cd45*$^{+}$ myeloid cluster (light green), a *Cd45*$^{+}$ lymphoid cluster (purple), a *Cd68*$^{+}$ cluster (dark green) or a *Ly6g*$^{+}$ neutrophil cluster (turquoise) from the unligated (UL) or ligated (L) side of long-term *EC-Prdm16*$^{+/+}$ (red lining) or *EC-Prdm16*$^{-/-}$ (dark pink lining) mice. (**F-J**) Diagram showing the quantification of Cd68^{+} cell recruitment around expanding collaterals in the adductor region of the ligated (L) and unligated (UL) side at 3 days (d) after femoral artery ligation in long-term *EC-Prdm16*$^{+/+}$ (*n*=9; red) or *EC-Prdm16*$^{-/-}$ (*n*=6; dark pink) mice (*F*) and representative pictures of cross-sections double-stained for α-smooth muscle cell actin (αSMA; in green) and Cd68 (in red) for each condition (*G-J*). Data represent mean ± SEM. **P*<0.05 *versus* indicated condition (Online Table III). Representative images for each condition represent the group average determined by the corresponding quantification. Scale bars: 50 μm in *G-J*.

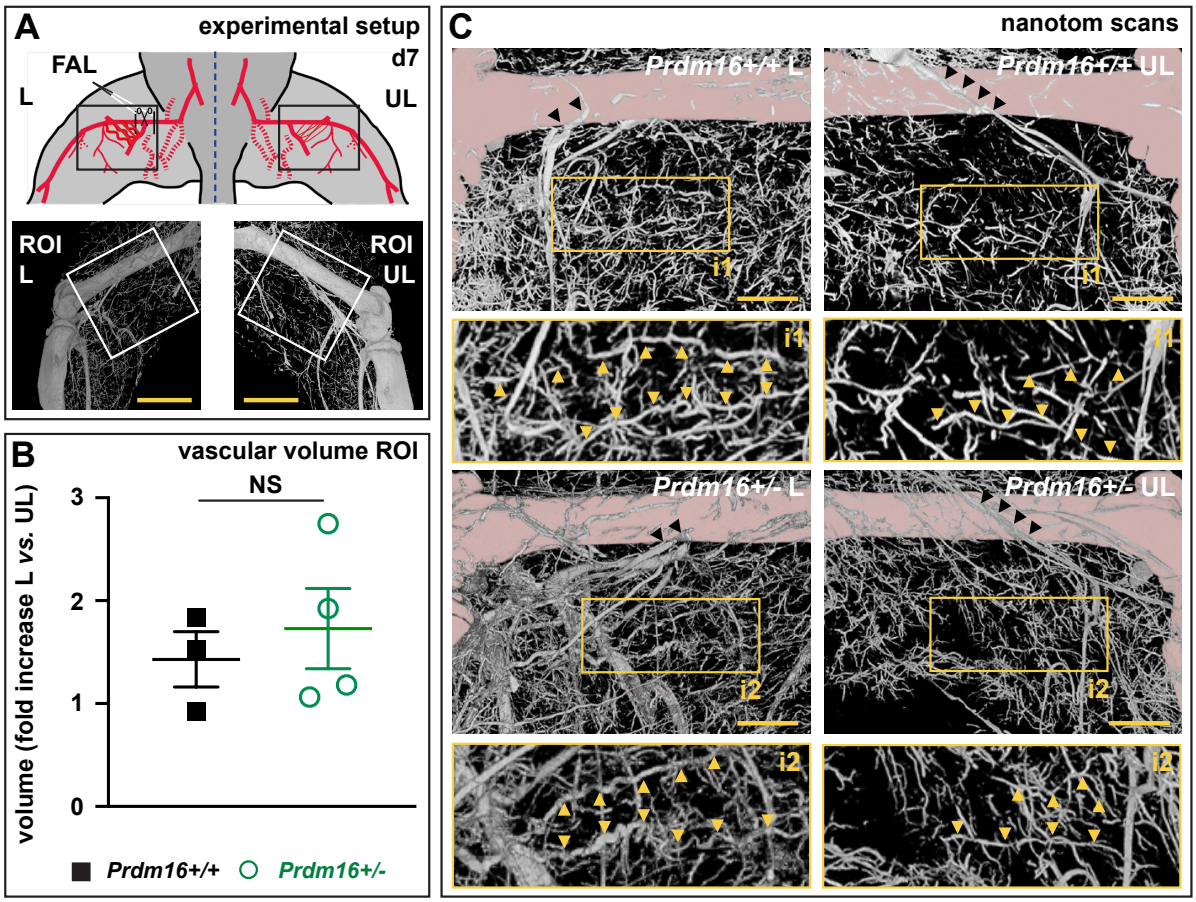

Online Figure VIII. ***Analysis of the vascular architecture in the adductor region by Nano-computed tomography (Nano-CT).*** **(A)** Diagram showing the experimental set-up indicating the region of interest (ROI) recorded on the unligated ('UL') and ligated ('L') side 7 days (d) after femoral artery ligation (FAL). **(B)** Diagram showing total vascular volume in the ROI on the UL and L side of *Prdm16*$^{+/-}$ mice (n=4) and their wild-type (n=3) littermates. Data are expressed as % ± SEM *versus* the UL side of *Prdm16*$^{+/+}$ mice (Online Table III). **(C)** Representative nano-CT angiograms of the UL (*right*) and L (*left*) side of a *Prdm16*$^{+/+}$ (*top*) or *Prdm16*$^{+/-}$ (*bottom*) mouse. Insets ('i') zoom in on the collaterals (yellow arrowheads). Black arrowheads show the interrupted and continuous femoral artery on the L and UL side, respectively. Bone is pseudo-colored in pink. Representative images for each condition represent the group average determined by the corresponding quantification. Scale bars: 4 mm (*A*), 2 mm (*C*).

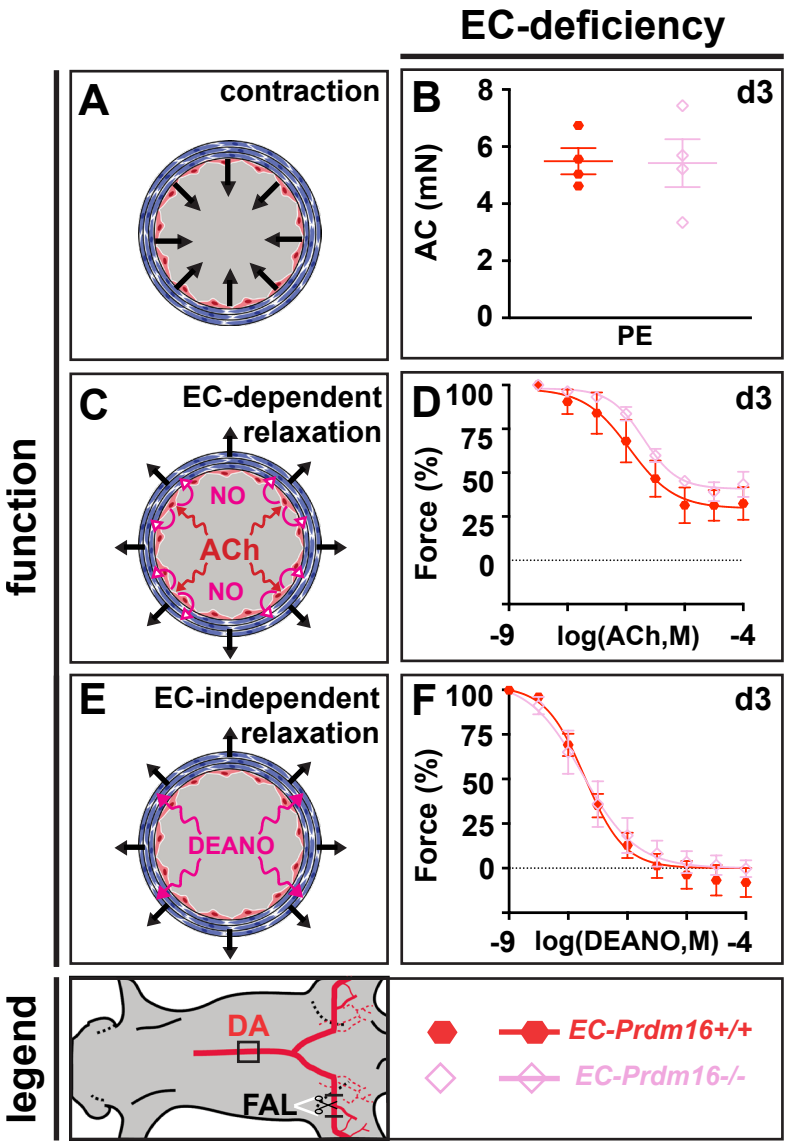

Online Figure IX. ***Long-term*** **Prdm16** ***deficiency in ECs does not affect vasomotor function in the descending aorta upstream from the ligation site.*** **(A,B)** Schematic representation (*A*) and quantification (*B*) of 3 x 10^{-6} mol/L phenylephrine (PE)-mediated absolute contraction (AC) in segments of the descending aorta (DA) 3 days (d) after femoral artery ligation (FAL) in long-term *EC-Prdm16*$^{+/+}$ (*n*=4) or *EC-Prdm16*$^{-/-}$ (*n*=4) mice. **(C,D)** Schematic representation (*C*) and quantification (*D*) of relative EC-dependent relaxation upon administration of acetylcholine (ACh) in the DA at d3 after FAL in long-term *EC-Prdm16*$^{+/+}$ (*n*=4) or *EC-Prdm16*$^{-/-}$ (*n*=4) mice. **(E,F)** Schematic representation (*E*) and quantification (*F*) of relative EC-independent relaxation upon administration of diethylamine NONOate (DEANO) in the DA at d3 after FAL in long-term *EC-Prdm16*$^{+/+}$ (*n*=4) or *EC-Prdm16*$^{-/-}$ (*n*=4) mice. Data represent mean ± SEM (Online Table III).

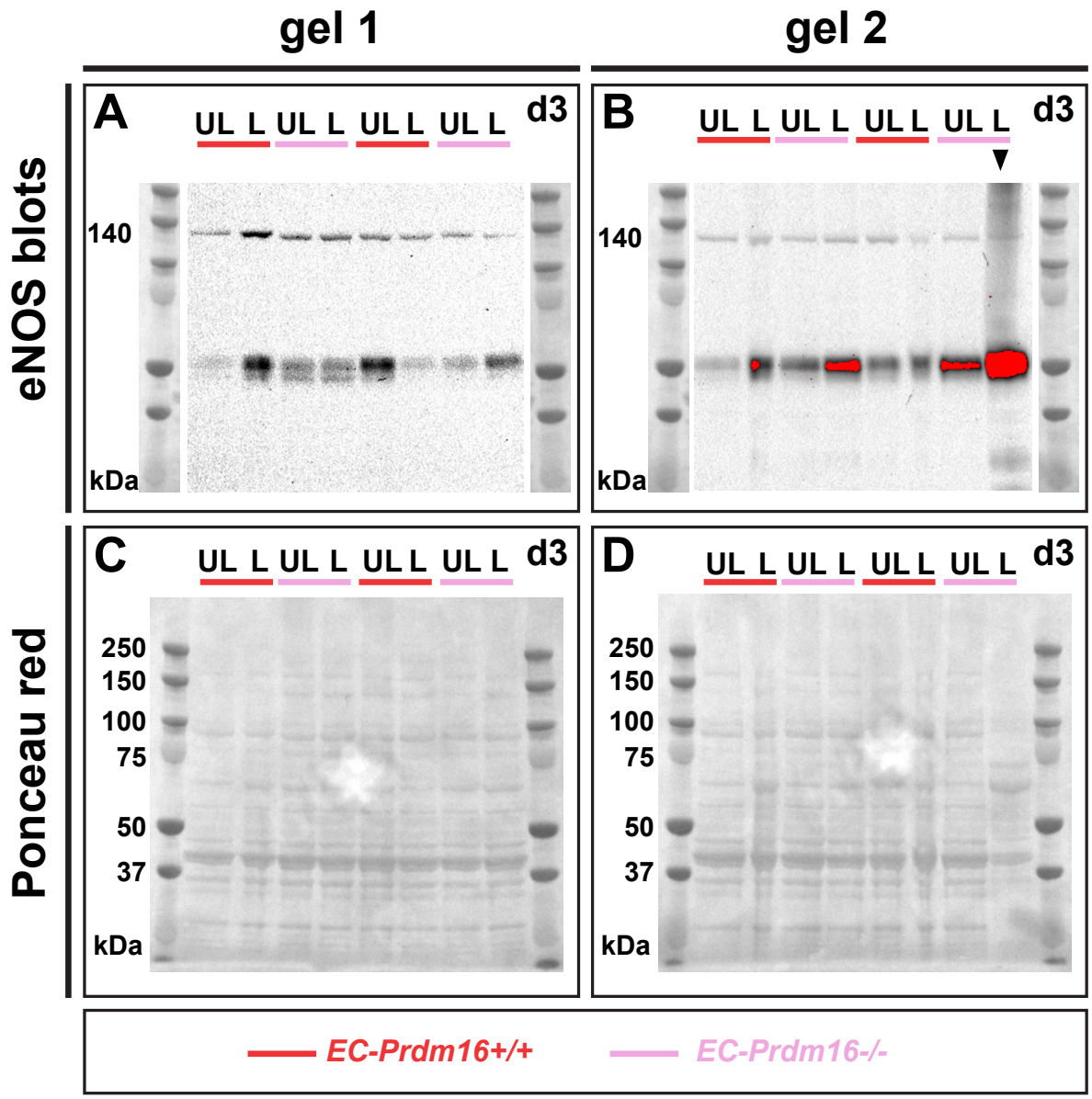

Online Figure X. ***Long-term* Prdm16 *deficiency in ECs does not affect eNOS protein expression upon HLI.*** **(A-D)** Western blots revealing eNOS protein (~140 kDa) expression (*A,B*) and corresponding loading control (Ponceau-stained gels; *C,D*) in the adductor region of long-term *EC-Prdm16*$^{+/+}$ (*n*=4) or *EC-Prdm16*$^{-/-}$ (*n*=4) mice 3 days (d) after femoral artery ligation. Molecular weight markers are indicated on each side of the gels. L: ligated side; UL: unligated side. One sample could not be reliably quantified due to the presence of a smear (panel *B*, lane N°8, indicated by arrowhead).

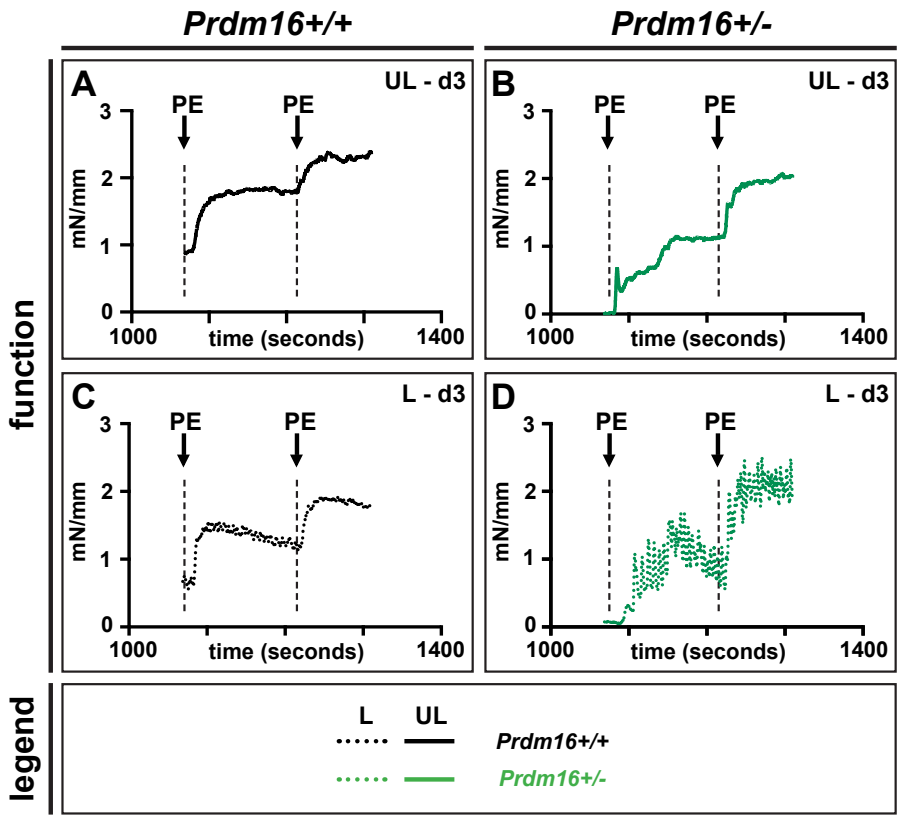

Online Figure XI. ***Contraction curves of*** **Prdm16$^{+/-}$** ***mice feature spikes upon HLI.*** **(A-D)** Representative dose-response curves of phenylephrine (PE)-mediated contraction of femoral artery (FA) segments from ligated (L) and unligated (UL) sides of *Prdm16*$^{+/+}$ and *Prdm16*$^{+/-}$ mice 3 days (d) after FA ligation. Normal contraction curves were observed in FA segments of the UL side of *Prdm16*$^{+/+}$ (*A*) and *Prdm16*$^{+/-}$ (*B*) mice. Subtle oscillations were observed in contraction curves of segments of the L side of *Prdm16*$^{+/+}$ mice (*C)* while contraction curves of segments of the L side of *Prdm16*$^{+/-}$ mice showed significant spikes (*D)*. UL and L segments of *Prdm16*$^{+/+}$ mice are represented by black full or dashed lines, respectively. UL and L segments of *Prdm16*$^{+/-}$ mice are represented by green full or dashed lines, respectively.

SUPPLEMENTAL TABLES

Online Table I. Major Resources Table

Genetically Modified Animals

Strain name	Species	Vendor or Source	Background Strain	Other Information	Persistent ID / URL
***Prdm16*$^{GT(OST67423)Lex}$**	mouse	Mutant Mouse Resource & Research Centers (MMRRC)	Backcrossed for 9 generations onto the C57Bl/6 genetic background		https://www.mmrrc.org/catalog/sds.php?mmrrc_id=11760
***Cdh5-Cre*^{ERT2}**	mouse	gift from R. Adams, Münster, Germany	C57Bl/6 background	now also commercially available at Taconic	Reference[18] https://www.taconic.com/mouse-model/cdh5pac-creert2-mouse
***Prdm16*$^{fl/fl}$**	mouse	gift from B. Spiegelman, Boston, USA	Backcrossed on a C57Bl/6 background	now also commercially available at the Jackson Laboratories	Reference[19] https://www.jax.org/strain/024992
Sm22α-Cre	mouse	gift from J. Herz, Texas, USA	Mixed CD1/C57Bl/6 background		Reference[20]

Antibodies

Target antigen	Vendor or Source	Catalog #	Working concentration (application)	Lot # (preferred but not required)	Persistent ID / URL
Prdm16	R&D Systems	AF6295	1:100 (IF)		https://www.rndsystems.com/products/human-mouse-prdm16-mel1-antibody_af6295
Sheep IgG	Jackson Immuno-research Labs	713-546-147	1:200 (IF)		https://www.jacksonimmuno.com/catalog/products/713-546-147
α-Smooth muscle actin	Sigma-Aldrich	C6198	1:1,000 (IF)		https://www.sigmaaldrich.com/content/dam/sigma-aldrich/docs/Sigma/Datasheet/3/c6198dat.pdf
Cd45	Beckton Dickinson	BD553081	1:100 (IF)		https://www.bdbiosciences.com/eu/applications/research/stem-cell-research/cancer-research/mouse/pe-rat-anti-mouse-cd45-30-f11/p/553081
Cd68	Abcam	ab125212	1:100 (IF)		https://www.abcam.com/cd68-antibody-ab125212.html
rabbit-IgG	Santa Cruz	Sc-2089	1:300 (IF)		https://datasheets.scbt.com/sc-2089.pdf
α-Smooth muscle actin	Sigma-Aldrich	F3777	1:200 (IF)		https://www.sigmaaldrich.com/catalog/product/sigma/f3777?lang=en&region=BE
Cd31	Beckton Dickinson	BD557355	1:500 (IF)		https://www.bdbiosciences.com/eu/applications/research/stem-cell-

					research/cancer-research/mouse/purified-rat-anti-mouse-cd31-mec-133/p/557355
Rat IgG	Invitrogen	A18919	1:500 (IF)		https://www.thermofisher.com/order/genome-database/dataSheetPdf?producttype=antibody&productsubtype=antibody_secondary&productId=A18919&version=117
eNOS	Beckton Dickinson	BD610297	1:2,000 (WB)		https://www.bdbiosciences.com/eu/reagents/research/antibodies-buffers/cell-biology-reagents/cell-biology-antibodies/purified-mouse-anti-enosnos-type-iii-3enosnos-type-iii/p/610297
Mouse IgG	Santa Cruz	sc-2314	1:2,000 (WB)		https://datasheets.scbt.com/sc-2314.pdf

Cultured Cells

Name	Vendor or Source	Sex (F, M, or unknown)	Persistent ID / URL
HUVECs	Generated in house	unknown	Not applicable

Data & Code Availability

Description	Source / Repository	Persistent ID / URL
scRNAseq dataset	scRNAseq data have been deposited in the ArrayExpress database at EMBL-EBI.	https://www.ebi.ac.uk/arrayexpress accession number E-MTAB-9703

Online Table II. List of primers for qRT-PCR

Gene	Forward primer (5'-3')	Reverse primer (5'-3')
	Mouse	
Hprt1	*CAGGCCAGACTTTGTTGGAT*	*TTGCGCTCATCTTAGGCTTT*
Prdm16	*CACGGAAGAGCGTGAGTACA*	*GGCAGACCTGCGATATGAAT*
Vegfa	*GGCCTCCGAAACCATGAACT*	*CTGCTCTCCTTCTGTCGTGG*
Nox2	*ACAGACTGCGGAGAGTTTGG*	*ACCTTGGGGCACTTGACAAA*
Nox4	*TGGCCAACGAAGGGGTTAAA*	*ACACAATCCTAGGCCCAACA*
Timp1	*GTAAGGCCTGTAGCTGTGCC*	*CGCTGGTATAAGGTGGTCTCG*
Timp4	*ACACGCCATTTGACTCTTCC*	*CAGCCACAGTTCTGGTGGTA*

Online Table III. Detailed statistics

Fig.	genotype	*n*	Parameter	Normal?*	Test/model	comparison	*P*-value
2B	*Prdm16+/+*	13	DA diameter	No	Mann-Whitney test	*Prdm16+/+ vs. +/-*	1.25E-02
	Prdm16+/-	14					
2C	*Prdm16+/+*	7	FA diameter	Yes	Student's *t*-test (unpaired)	*Prdm16+/+ vs. +/-*	4.09E-02
	Prdm16+/-	8					
2E	*Prdm16+/+*	7	DA SMC coating	Yes	Student's *t*-test (unpaired)	*Prdm16+/+ vs. +/-*	1.88E-01
	Prdm16+/-	8					
2F	*Prdm16+/+*	7	FA SMC coating	Yes	Student's *t*-test (unpaired)	*Prdm16+/+ vs. +/-*	1.97E-02
	Prdm16+/-	8					
2H	*Prdm16+/+*	5	Aortic response to PE (concentration: $3x10^{-6}$ mol/L)	Yes	Student's *t*-test (unpaired)	*Prdm16+/+ vs. +/-*	2.30E-01
	Prdm16+/-	6					
2I	*Prdm16+/+*	7		Yes	Student's *t*-test (unpaired)	*Prdm16+/+ vs. +/-*	4.63E-01
	Prdm16+/-	7					
Suppl. IXB	*LT EC-Prdm16+/+*	4		NV**	Mann-Whitney test	*LT EC-Prdm16+/+ vs. -/-*	8.86E-01
	LT EC-Prdm16-/-	4					
2K	*Prdm16+/+*	6	Aortic response to increasing dose of Ach (1.1 to 1.8 or 1.9 correspond to rising concentration)	Yes***	RM 2-way ANOVA (Bonferroni post-hoc test)	*Prdm16+/+ vs. +/-*	1.1) 4.09E-01 1.2) to 1.8): >9.99E-01
	Prdm16+/-	5					
2L	*Prdm16+/+*	7		Yes***	RM 2-way ANOVA (Bonferroni post-hoc test)	*Prdm16+/+ vs. +/-*	1.1) to 1.9): >9.99E-01
	Prdm16+/-	7					
Suppl. IXD	*LT EC-Prdm16+/+*	4		Yes***	RM 2-way ANOVA (Bonferroni post-hoc test)	*LT EC-Prdm16+/+ vs. -/-*	1.1) to 1.8): >9.99E-01
	LT EC-Prdm16-/-	4					
2N	*Prdm16+/+*	6	Aortic response to increasing dose of Ach (+DEANO) (1.1 to 1.10 or 1.11 correspond to rising concentration)	Yes***	RM 2-way ANOVA (Bonferroni post-hoc test)	*Prdm16+/+ vs. +/-*	1.1) to 1.10): >9.99E-01
	Prdm16+/-	6					
2O	*Prdm16+/+*	7		Yes***	RM 2-way ANOVA (Bonferroni post-hoc test)	*Prdm16+/+ vs. +/-*	1.1) to 1.11): >9.99E-01
	Prdm16+/-	7					
Suppl. IXF	*LT EC-Prdm16+/+*	4		Yes***	RM 2-way ANOVA (Bonferroni post-hoc test)	*LT EC-Prdm16+/+ vs. -/-*	1.1) to 1.10): >9.99E-01
	LT EC-Prdm16-/-	4					
3B	*Prdm16+/+*	12	Arterial flow recovery (time points day (d) 0 to d21)	Yes***	RM 2-way ANOVA (Bonferroni post-hoc test)	*Prdm16+/+ vs. +/-*	d0: >9.99E-01 d3: >9.99E-01 d7: 1.16E-01 d10: 2.25E-02 d14: >9.99E-01 d21: 2.60E-04
	Prdm16+/-	12					
3F	*LT EC-Prdm16+/+*	12		Yes***	RM 2-way ANOVA (Bonferroni post-hoc test)	*LT EC-Prdm16+/+ vs. -/-*	d0: 1.35E-01 d3: 7.87E-04 d7: 1.62E_02 d10: 1.79E-01 d14: >9.99E-01 d21: 3.29E-03
	LT EC-Prdm16-/-	10					
3J	*ST EC-Prdm16+/+*	16		Yes***	RM 2-way ANOVA (Bonferroni post-hoc test)	*ST EC-Prdm16+/+ vs. -/-*	d0: >9.99E-01 d3: >9.99E-01 d7: >9.99E-01 d10: >9.99E-01 d14: 8.9E-01 d21: 1.65E-03
	ST EC-Prdm16-/-	13					
3N	*SMC-Prdm16+/+*	8		Yes***	RM 2-way ANOVA (Bonferroni post-hoc test)	*SMC-Prdm16+/+ vs. -/-*	d0: 6.38E-02 d3: 1.25E-01 d7: 2.93E-01 d10: >9.99E-01 d14: >9.99E-01 d21: 3.5E-01
	SMC-Prdm16-/-	10					
3C	*Prdm16+/+*	12	Necrosis (time points day (d) 0 to d21)	non-continuous (ordinal)	Cumulative link mixed model for ordinal data	*Prdm16+/+ vs. +/-*	3.11E-03 *P*-value for group effect
	Prdm16+/-	12					
3G	*LT EC-Prdm16+/+*	12				*LT EC-Prdm16+/+ vs. -/-*	2.63E-03

	LT EC-Prdm16-/-	10		non-continuous (ordinal)	Cumulative link mixed model for ordinal data		*P*-value for group effect
3K	*ST EC-Prdm16+/+*	16		non-continuous (ordinal)	Cumulative link mixed model for ordinal data	*ST EC-Prdm16+/+ vs. -/-*	8.32E-02 *P*-value for group effect
	ST EC-Prdm16-/-	13					
3O	*SMC-Prdm16+/+*	8		non-continuous (ordinal)	Cumulative link mixed model for ordinal data	*SMC-Prdm16+/+ vs. -/-*	1.50E-01 *P*-value for group effect
	SMC-Prdm16-/-	10					
3D	*Prdm16+/+*	8	Fibrosis (day 21)	Yes	unpaired Student's *t*-test	*Prdm16+/+ vs. +/-*	1.50E-02
	Prdm16+/-	8					
3H	*LT EC-Prdm16+/+*	11		Yes	unpaired Student's *t*-test	*LT EC-Prdm16+/+ vs. -/-*	1.45E-06
	LT EC-Prdm16-/-	9					
3L	*ST EC-Prdm16+/+*	10		Yes	unpaired Student's *t*-test	*ST EC-Prdm16+/+ vs. -/-*	8.98E-04
	ST EC-Prdm16-/-	10					
3P	*SMC-Prdm16+/+*	8		Yes	unpaired Student's *t*-test	*SMC-Prdm16+/+ vs. -/-*	3.07E-01
	SMC-Prdm16-/-	10					
4B *****	*Prdm16+/+ UL*	5	$CD45^+$ cell recruitment around collaterals (day 3)	Yes****	2-way ANOVA (Bonferroni post-hoc test)	*1)Prdm16+/+ UL vs. +/- UL* *2) Prdm16+/+ UL vs. +/+ L* *3) Prdm16+/- UL vs. +/- L* *4) Prdm16+/+ L vs. +/- L*	1) >9.99E-01 2) 3.05E-02 3)1.18E-03 4) 9.96E-02
	Prdm16+/- UL	3					
	Prdm16+/+ L	5					
	Prdm16+/- L	3					
4C *****	*LT EC-Prdm16+/+ UL*	8		Yes	2-way ANOVA (Bonferroni post-hoc test)	1) *LT EC-Prdm16+/+ UL vs.+/- UL* 2) *LT EC-Prdm16+/+ UL vs. +/+ L* 3) *LT EC-Prdm16-/- UL vs. -/- L* 4) *LT EC-Prdm16+/+ L vs. -/- L*	1) >9.99E-01 2) 1.73E-02 3) 7.43E-02 4) >9.99E-01
	LT EC-Prdm16-/- UL	5					
	LT EC-Prdm16+/+ L	8					
	LT EC-Prdm16-/- L	5					
Suppl. VIIF *****	*LT EC-Prdm16+/+UL*	9	$CD68^+$ cell recruitment around collaterals (day 3)	Yes	2-way ANOVA (Bonferroni post-hoc test)	1) *LT EC-Prdm16+/+ UL vs. -/- UL* 2) *LT EC-Prdm16+/+ UL vs. +/+ L* 3) *LT EC-Prdm16-/- UL vs. -/- L* 4) *LT EC-Prdm16+/+ L vs. -/- L*	1) >9.99E-01 2) 1.53E-01 3) 1.04E-02 4) 5.21E-01
	LT EC-Prdm16-/-UL	6					
	LT EC-Prdm16+/+ L	9					
	LT EC-Prdm16-/- L	6					
4E *****	*Prdm16+/+ UL*	8	Collateral diameter (day 21)	Yes	2-way ANOVA (Bonferroni post-hoc test)	*1)Prdm16+/+ UL vs. +/- UL* *2) Prdm16+/+ UL vs. +/+ L* *3) Prdm16+/- UL vs. +/- L* *4) Prdm16+/+ L vs. +/- L*	1) 1.99E-01 2) >9.99E-01 3) 5.36E-03 4) >9.99E-01
	Prdm16+/- UL	8					
	Prdm16+/+ L	8					
	Prdm16+/- L	8					
4F *****	*LT EC-Prdm16+/+ UL*	11		Yes	2-way ANOVA (Bonferroni post-hoc test)	1) *LT EC-Prdm16+/+ UL vs. -/- UL* 2) *LT EC-Prdm16+/+ UL vs. +/+ L* 3) *LT EC-Prdm16-/- UL vs. -/- L* 4) *LT EC-Prdm16+/+ L vs. -/- L*	1) >9.99E-01 2) 2.67E-06 3) 2.79E-05 4) >9.99E-01
	LT EC-Prdm16-/- UL	8					
	LT EC-Prdm16+/+ L	11					
	LT EC-Prdm16-/- L	8					
4H *****	*Prdm16+/+ UL*	7	Collateral SMC coating (day 21)	Yes	2-way ANOVA (Bonferroni post-hoc test)	*1) Prdm16+/+ UL vs. +/- UL* *2)Prdm16+/+ UL vs. +/+ L* *3) Prdm16+/- UL vs. +/- L* *4) Prdm16+/+ L vs. +/- L*	1) >9.99E-01 2) 3.01E-01 3) 1.88E-01 4) >9.99E-01
	Prdm16+/- UL	8					
	Prdm16+/+ L	7					
	Prdm16+/- L	8					

4I *****	*LT EC-Prdm16+/+ UL*	11		Yes	2-way ANOVA (Bonferroni post-hoc test)	1) *LT EC-Prdm16+/+ UL vs. -/- UL* 2) *LT EC-Prdm16+/+ UL vs. +/+ L* 3) *LT EC-Prdm16-/- UL vs. -/- L* 4) *LT EC-Prdm16+/+ L vs. -/- L*	1) >9.99E-01 2) 1.20E-06 3) 1.10E-06 4) >9.99E-01
	LT EC-Prdm16-/- UL	8					
	LT EC-Prdm16+/+ L	11					
	LT EC-Prdm16-/- L	8					
4K *****	*Prdm16+/+ UL*	6	Capillary density gastrocnemius (day 21)	Yes	2-way ANOVA (Bonferroni post-hoc test)	*1) Prdm16+/+ UL vs. +/- UL* *2)Prdm16+/+ UL vs. +/+ L* *3) Prdm16+/-UL vs. +/- L* *4) Prdm16+/+ L vs. +/- L*	1) >9.99E-01 2) >9.99E-01 3) 4.33E-07 4) 1.38E-06
	Prdm16+/- UL	6					
	Prdm16+/+ L	6					
	Prdm16+/- L	6					
4L *****	*LT EC-Prdm16+/+ UL*	12		Yes	2-way ANOVA (Bonferroni post-hoc test)	1) *LT EC-Prdm16+/+ UL vs. -/- UL* 2) *LT EC-Prdm16+/+ UL vs. +/+ L* 3) *LT EC-Prdm16-/- UL vs. -/- L* 4) *LT EC-Prdm16+/+ L vs. -/- L*	1) >9.99E-01 2) >9.99E-01 3) 2.99E-11 4) 7.22E-11
	LT EC-Prdm16-/- UL	9					
	LT EC-Prdm16+/+ L	12					
	LT EC-Prdm16-/- L	9					
5B *****	*Prdm16+/+ UL*	7	Aortic response to increasing dose of PE (x.1 to x.9 correspond to rising concentration)	Yes***	RM ANOVA (Bonferroni post-hoc test)	*1) Prdm16+/+ UL vs. +/- UL* *2)Prdm16+/+ UL vs. +/+ L* *3) Prdm16+/- UL vs. +/- L* *4) Prdm16+/+ L vs. +/- L*	1.1) to 1.7) >9.99E-01 1.8) 6.97E-01 1.9) >9.99E-01 2.1) to 2.5) >9.99E-01 2.6) 6.43E-01 2.7) 1.73E-01 2.8) 8.91E-02 2.9) 9.64E-02 3.1) to 3.5) >9.99E-01 3.6) 4.08E-01 3.7) 1.27E-01 3.8) 2.56E-02 3.9) 1.54E-02 4.1) to 4.7) >9.99E-01 4.8) 1.55E-01 4.9) 1.71E-01
	Prdm16+/- UL	6					
	Prdm16+/+ L	7					
	Prdm16+/- L	5					
5C *****	*LT EC-Prdm16+/+ UL*	5		Yes***	RM ANOVA (Bonferroni post-hoc test)	1) *LT EC-Prdm16+/+ UL vs. -/- UL* 2) *LT EC-Prdm16+/+ UL vs. +/+ L* 3) *LT EC-Prdm16-/- UL vs. -/- L* 4) *LT EC-Prdm16+/+ L vs. -/- L*	1.1) to 1.4) >9.99E-01 1.5) 4.78E-01 1.6) to 1.9) >9.99E-01 2.1) to 2.7) >9.99E-01 2.8) 5.11E-01 2.9) 4.13E-01 3.1) to 3.6) >9.99E-01 3.7) 8.54E-01 3.8) 1.33E-01 3.9) 3.19E-01 4.1) to 4.9): >9.99E-01
	LT EC-Prdm16-/- UL	5					
	LT EC-Prdm16+/+ L	3					
	LT EC-Prdm16-/- L	4					
5E *****	*Prdm16+/+ UL*	7	Aortic response to increasing dose of Ach (x.1 to x.8 correspond to rising concentration)	Yes***	RM ANOVA (Bonferroni post-hoc test)	*1) Prdm16+/+ UL vs. Prdm16+/- UL* *2)Prdm16+/+ UL vs. Prdm16+/+ L* *3) Prdm16+/- UL vs. Prdm16+/- L* *4) Prdm16+/+ L vs. Prdm16+/- L*	1.1) to 1.8): >9.99E-01 2.1) >9.99E-01 2.2) 1.07E-01 2.3) 2.99E-02 2.4) to 2.8) >9.99E-01 3.1) >9.99E-01 3.2) 5.24E-01 3.3) 1.69E-01 3.4) to 3.8) >9.99E-01 4.1) to 4.8): >9.99E-01
	Prdm16+/+ UL	7					
	Prdm16+/- UL	6					
	Prdm16+/+ L	7					
	Prdm16+/- L	5					

5F *****	*LT EC-Prdm16+/+ UL*	5		Yes***	RM ANOVA (Bonferroni post-hoc test)	1) *LT EC-Prdm16+/+ UL vs. -/- UL* 2) *LT EC-Prdm16+/+ UL vs. +/+ L* 3) *LT EC-Prdm16-/- UL vs. -/- L* 4) *LT EC-Prdm16+/+ L vs. -/- L*	1.1) to 1.8): >9.99E-01 2.1) to 2.8: >9.99E-01 3.1) to 3.3) >9.99E-01 3.4) 1.96E-01 3.5) 1.97E-02 3.6) 1.59E-03 3.7) 1.42E-02 3.8) 2.33E-02 4.1) >9.99E-01 4.2) >9.99E-01 4.3) 6.25E-01 4.4) 3.82E-01 4.5) 5.37E-01 4.6) 3.35E-01 4.7) 9.21E-01 4.8) >9.99E-01
	LT EC-Prdm16-/- UL	5					
	LT EC-Prdm16+/+ L	3					
	LT EC-Prdm16-/- L	4					
5H *****	*Prdm16+/+ UL*	7	Aortic response to increasing dose of Ach (+DEANO) (x.1 to x.10 correspond to rising concentration)	Yes***	RM ANOVA (Bonferroni post-hoc test)	*1) Prdm16+/+ UL vs. +/- UL* *2)Prdm16+/+ UL vs. +/+ L* *3) Prdm16+/- UL vs. +/- L* *4) Prdm16+/+ L vs. +/- L*	1.1) to 1.4) >9.99E-01 1.5) 6.03E-01 1.6) to 1.10) >9.99E-01 2.1) to 2.4) >9.99E-01 2.5) 2.86E-04 2.6) 6.01E-02 2.7) to 2.10) >9.99E-01 3.1) to 3.3) >9.99E-01 3.4) 1.17E-01 3.5) to 3.10) >9.99E-01 4.1) to 4.10): >9.99E-01
	Prdm16+/- UL	6					
	Prdm16+/+ L	7					
	Prdm16+/- L	5					
5I *****	*LT EC-Prdm16+/+ UL*	5		Yes***	RM ANOVA (Bonferroni post-hoc test)	1) *LT EC-Prdm16+/+ UL vs. -/- UL* 2) *LT EC-Prdm16+/+ UL vs. +/+ L* 3) *LT EC-Prdm16-/- UL vs. -/- L* 4) *LT EC-Prdm16+/+ L vs. -/- L*	1.1) to 1.4) >9.99E-01 1.5) 1.34E-01 1.6) 9.60E-02 1.7) to 1.10) >9.99E-01 2.1) to 2.4) >9.99E-01 2.5) 1.69E-01 2.6) 3.60E-01 2.7) to 2.10) >9.99E-01 3.1) to 3.4) >9.99E-01 3.5) 1.51E-01 3.6) 8.76E-02 3.7) to 3.10) >9.99E-01 4.1) >9.99E-01 4.2) >9.99E-01 4.3) 3.55E-01 4.4) >9.99E-01 4.5) 1.79E-01 4.6) 3.08E-01 4.7) to 4.10) >9.99E-01
	LT EC-Prdm16-/- UL	5					
	LT EC-Prdm16+/+ L	3					
	LT EC-Prdm16-/- L	4					
7A	Cherry	12	ionomycin	Yes	Paired Student's *t*-test	Cherry *vs.* Prdm16	1.16E-05
	Prdm16	12					
7B	Cherry	8	thapsigargin	Yes	Paired Student's *t*-test	Cherry *vs.* Prdm16	7.58E-01
	Prdm16	8					
7C	Cherry	8	SOCE	Yes	Paired Student's *t*-test	Cherry *vs.* Prdm16	1.14E-04
	Prdm16	8					
7D	*LT EC-Prdm16+/+*	7	Quantitative RT-PCR for *Nox* genes	Yes	Unpaired Student's *t*-test	*LT EC-Prdm16+/+ vs. -/-*	1.09E-01
	LT EC-Prdm16-/-	7					

7E	*LT EC-Prdm16+/+*	6		Yes	Unpaired Student's *t*-test	*LT EC-Prdm16+/+ vs. -/-*	3.87E-02
	LT EC-Prdm16-/-	7					
Suppl. IE	*LT EC-Prdm16+/+*	3	Recombination efficiency	NV**	Mann-Whitney test	*LT EC-Prdm16+/+ vs. -/-*	1.00E-01
	LT EC-Prdm16-/-	3					
Suppl. IF	*ST EC-Prdm16+/+*	4		NV**	Mann-Whitney test	*ST EC-Prdm16+/+ vs. -/-*	5.71E-02
	ST EC-Prdm16-/-	3					
Suppl. IVB	*Prdm16+/+*	6	Compliance	Yes	Unpaired Student's *t*-test	*Prdm16+/+ vs. +/-*	5.51E-01
	Prdm16+/-	6					
Suppl. IVC	*Prdm16+/+*	6	Peterson's modulus	No	Mann-Whitney test	*Prdm16+/+ vs. +/-*	6.99E-01
	Prdm16+/-	6					
Suppl. VE	*Prdm16+/+*	8	Fibro-adipose tissue (day 21)	No	Mann-Whitney test	*Prdm16+/+ vs. +/-*	3.11E-04
	Prdm16+/-	7					
Suppl. VJ	*LT EC-Prdm16+/+*	11		No	Mann-Whitney test	*LT EC-Prdm16+/+ vs. -/-*	7.74E-04
	LT EC-Prdm16-/-	10					
Suppl. VO	*ST EC-Prdm16+/+*	11		No	Mann-Whitney test	*ST EC-Prdm16+/+ vs. -/-*	2.09E-02
	ST EC-Prdm16-/-	10					
Suppl. VT	*SMC-Prdm16+/+*	9		No	Mann-Whitney test	*SMC-Prdm16+/+ vs. -/-*	7.37E-01
	SMC-Prdm16-/-	11					
Suppl. VIIIB	*Prdm16+/+*	3	Vascular volume (nano-CT)	NV**	Mann-Whitney test	*Prdm16+/+ vs. +/-*	6.29E-01
	Prdm16+/-	4					

*data distribution was determined separately for each group of each experiment (reported in the corresponding Figure panel in column 1) by Kolmogorov-Smirnov test (if group size '*n*' was ≥ 5 and < 8) or by D'Agostino & Pearson test (if group size was ≥ 8); if all groups of an experiment were normally distributed (as indicated by 'Yes' in column 5) a parametric test was used, otherwise ('No' in column 5) a non-parametric test was used;

**when normality could not be verified ('NV' in column 5) based on the abovementioned tests (*i.e.*, size of at least one of the groups was < 5), a non-parametric test was used;

***for repeated measurements ANOVA models, only random effects and residuals were assumed to have a normal distribution;

****here we used a parametric test as we assume normality of the datasets based on the fact that the type of parameter ($CD45^+$ cell recruitment around collaterals) and experimental set-up was the same as for **4C** for which the datasets were normally distributed for all groups based on the abovementioned tests;

*****only the *P*-values for the 4 biologically relevant group comparisons are mentioned although *P*-value correction was performed for all 6 possible comparisons.

Abbreviations: Suppl.: supplementary online; EC: endothelial cell; SMC: smooth muscle cell; PE: phenylephrine; Ach: acetylcholine; DEANO: diethylamine NONOate; LT: long-term; ST: short-term; L: ligated; UL: unligated; SOCE: store-operated calcium entry; CT: computed tomography.

Online Table IV. Type B1 genes (*n*= 217) uniquely altered by FAL in *EC-Prdm16*$^{+/+}$ mice

Gene name	Average LogFc L *vs.* UL	pct L	pct UL	Δpct L-UL	Adjusted *P*-value
A4galt	-0.51	0.009	0.238	-0.229	3.38E-02
Ace	-0.35	0.036	0.302	-0.266	4.06E-02
Adam17	-0.46	0.009	0.238	-0.229	3.63E-02
Aggf1	-0.78	0.062	0.397	-0.335	5.56E-03
Ankrd17	-0.69	0.018	0.333	-0.315	2.73E-04
Ap2a1	**-0.35**	**0.018**	**0.270**	**-0.252**	**1.68E-02**
Ap3b1	-0.39	0.009	0.254	-0.245	1.12E-02
Arglu1	-0.77	0.062	0.413	-0.351	2.43E-03
Arhgap29	-0.48	0.125	0.460	-0.335	1.95E-02
Arhgdia	-0.35	0.250	0.619	-0.369	7.29E-03
Arl6ip5	-0.50	0.054	0.349	-0.295	4.37E-02
Ash1l	-0.70	0.045	0.397	-0.352	5.02E-04
Ass1	-0.76	0.027	0.302	-0.275	1.75E-02
Atp1a1	**-0.44**	**0.116**	**0.508**	**-0.392**	**1.70E-04**
Atp6v1g1	-0.33	0.188	0.524	-0.336	1.32E-02
Atraid	-0.50	0.080	0.444	-0.364	1.35E-03
Azin1	-0.78	0.054	0.365	-0.311	1.75E-02
Cbfa2t3	-0.44	0.045	0.333	-0.288	1.76E-02
Cd59a	-0.91	0.009	0.381	-0.372	5.30E-07
Cds2	-0.66	0.009	0.254	-0.245	9.29E-03
Cgnl1	-1.15	0.027	0.302	-0.275	1.44E-02
Chd2	-0.38	0	0.190	-0.190	1.13E-02
Clstn1	-0.46	0.027	0.302	-0.275	1.87E-02
Cltc	**-0.40**	**0.134**	**0.476**	**-0.342**	**1.74E-02**
Col8a1	-0.94	0.054	0.349	-0.295	3.42E-02
Copa	-0.36	0.080	0.413	-0.333	4.50E-03
Cox5b	-0.34	0.196	0.571	-0.375	5.07E-03
Cox6a1	-0.32	0.196	0.571	-0.375	2.82E-03
Cpd	-0.71	0.045	0.381	-0.336	1.56E-03
Crlf2	-0.59	0.036	0.317	-0.281	3.04E-02
Ctnnb1	-0.81	0.107	0.571	-0.464	4.82E-06
Cyc1	-0.52	0.071	0.413	-0.342	1.22E-03
Cyth3	-0.97	0.018	0.333	-0.315	2.83E-04
Dad1	-0.49	0.143	0.492	-0.349	3.21E-02
Dctn2	-0.42	0.080	0.397	-0.317	3.96E-02
Ddx17	-0.34	0.125	0.460	-0.335	3.65E-02
Dennd5b	-0.82	0.036	0.349	-0.313	2.92E-03
Dgcr2	-0.37	0	0.190	-0.190	1.13E-02
Diaph2	-0.52	0.036	0.349	-0.313	3.22E-03
Dlc1	-0.72	0.027	0.317	-0.290	5.22E-03
Dlst	-0.50	0	0.222	-0.222	1.01E-03
Dmd	-0.60	0.009	0.238	-0.229	3.27E-02
Dnaja1	**-0.63**	**0.241**	**0.635**	**-0.394**	**1.77E-02**

Gene name	Average LogFc L *vs.* UL	pct L	pct UL	Δpct L-UL	Adjusted *P*-value
Dnajc3	-0.51	0.036	0.349	-0.313	2.26E-03
Dock6	-0.36	0.054	0.349	-0.295	3.04E-02
Dock9	-0.71	0.036	0.365	-0.329	1.09E-03
Dync1i2	-0.44	0.080	0.444	-0.364	8.59E-04
Eepd1	-0.42	0	0.175	-0.175	3.69E-02
Efhd1	-0.54	0.009	0.238	-0.229	1.75E-02
Eif4a2	-0.49	0.143	0.508	-0.365	8.45E-03
Elk3	-0.29	0.116	0.429	-0.313	3.53E-02
Eng	-0.39	0.188	0.571	-0.383	1.67E-03
Entpd1	-0.67	0.054	0.381	-0.327	4.14E-03
Ergic2	-0.39	0.027	0.302	-0.275	1.77E-02
Esyt2	-0.64	0.018	0.333	-0.315	2.98E-04
Exoc3	-0.37	0.018	0.286	-0.268	9.83E-03
Ext2	-0.53	0.009	0.302	-0.293	3.33E-04
F11r	-1.04	0.054	0.492	-0.438	1.22E-06
Fermt2	-0.48	0.098	0.444	-0.346	1.42E-02
Fez2	-0.79	0.027	0.333	-0.306	2.05E-03
Flna	-0.56	0.071	0.381	-0.310	2.37E-02
Flnb	-0.78	0.062	0.381	-0.319	1.92E-02
Fnta	-0.44	0.018	0.302	-0.284	3.21E-03
Fryl	-0.72	0.054	0.429	-0.375	5.32E-05
Fstl1	-0.59	0.080	0.397	-0.317	4.97E-02
Gjc1	-0.34	0	0.190	-0.190	1.13E-02
Gna11	**-0.58**	**0.071**	**0.429**	**-0.358**	**1.33E-03**
Gnaq	**-0.43**	**0.062**	**0.365**	**-0.303**	**2.37E-02**
Gpatch8	-0.44	0.018	0.270	-0.252	2.67E-02
Gpd2	-0.41	0	0.206	-0.206	3.40E-03
Hdgfl3	-0.55	0.018	0.270	-0.252	2.85E-02
Hip1r	**-0.39**	**0**	**0.222**	**-0.222**	**1.01E-03**
Hnrnph1	-0.61	0.045	0.365	-0.320	3.34E-03
Hsd17b11	-0.72	0.009	0.254	-0.245	1.11E-02
Hspa5	-0.61	0.107	0.508	-0.401	2.23E-04
Ifi27	-0.43	0.152	0.508	-0.356	1.30E-02
Ifitm2	-0.46	0.384	0.778	-0.394	2.69E-02
Ik	-0.26	0.036	0.317	-0.281	1.17E-02
Itgb5	-0.38	0	0.206	-0.206	3.40E-03
Jag2	-0.74	0	0.317	-0.317	5.40E-07
Kank2	-0.49	0	0.238	-0.238	2.99E-04
Kidins220	-0.40	0.009	0.238	-0.229	3.63E-02
Kif1b	-0.31	0.027	0.302	-0.275	1.34E-02
Kif5b	-0.51	0.107	0.524	-0.417	8.41E-05
Klf13	-0.40	0.134	0.492	-0.358	5.92E-03
Kmt2e	-0.59	0.098	0.476	-0.378	1.47E-03
Krtcap2	-0.39	0.196	0.587	-0.391	7.57E-04

Gene name	Average LogFc L *vs.* UL	pct L	pct UL	Δpct L-UL	Adjusted *P*-value
Lamp2	-0.45	0.071	0.381	-0.310	2.70E-02
Lmo1	-0.57	0.098	0.429	-0.331	3.57E-02
Lyst	-0.45	0	0.190	-0.190	1.13E-02
Mageh1	-0.30	0	0.190	-0.190	1.13E-02
Magt1	-0.61	0.009	0.254	-0.245	1.15E-02
Manf	-0.52	0.062	0.413	-0.351	1.32E-03
Map7d1	-0.62	0.045	0.333	-0.288	3.83E-02
Mar-06	-0.49	0.009	0.238	-0.229	3.63E-02
Mat2a	-0.70	0.071	0.413	-0.342	7.00E-03
Matr3	-0.43	0.045	0.397	-0.352	1.15E-04
Mecom	-0.87	0.080	0.460	-0.380	6.76E-04
Mfap5	-0.72	0	0.238	-0.238	2.99E-04
Mfsd6	-0.50	0.018	0.286	-0.268	6.42E-03
Mllt6	-0.45	0	0.175	-0.175	3.69E-02
Mob2	-0.95	0.027	0.397	-0.370	1.64E-05
Mprip	-0.67	0.071	0.397	-0.326	1.90E-02
Mrpl42	-0.47	0.045	0.349	-0.304	8.88E-03
Mxd4	-0.28	0.143	0.476	-0.333	3.34E-02
Myl12b	-0.36	0.170	0.540	-0.370	6.57E-03
Myo10	-0.28	0.054	0.333	-0.279	1.40E-02
Nckap1	-0.79	0.071	0.444	-0.373	8.12E-04
Ndel1	-0.39	0.027	0.286	-0.259	3.93E-02
Ndufa1	-0.31	0.170	0.508	-0.338	2.54E-02
Ndufb7	-0.31	0.179	0.524	-0.345	9.72E-03
Nenf	-0.62	0.080	0.492	-0.412	1.77E-05
Nfix	-0.52	0.089	0.413	-0.324	3.15E-02
Nol7	-0.38	0.125	0.476	-0.351	9.40E-03
Notch1	-0.53	0.054	0.397	-0.343	8.91E-04
Pbrm1	-0.62	0.054	0.349	-0.295	3.85E-02
Pdcd5	-0.26	0.107	0.444	-0.337	5.56E-03
Pdgfb	**-0.84**	**0.045**	**0.444**	**-0.399**	**8.43E-06**
Pdlim5	-0.43	0.045	0.333	-0.288	1.24E-02
Peak1	-0.63	0	0.222	-0.222	1.01E-03
Picalm	**-0.54**	**0.071**	**0.381**	**-0.310**	**4.00E-02**
Pigt	-0.36	0.027	0.302	-0.275	1.01E-02
Pikfyve	-0.32	0	0.190	-0.190	1.13E-02
Pkd1	-0.60	0.036	0.317	-0.281	3.04E-02
Pkn2	-0.32	0.036	0.317	-0.281	2.10E-02
Plxnd1	-0.44	0.116	0.460	-0.344	1.42E-02
Pmepa1	-0.66	0.054	0.365	-0.311	1.25E-02
Pon2	-0.56	0.036	0.333	-0.297	9.45E-03
Ppp1r12a	-0.75	0.062	0.429	-0.367	7.57E-04
Ppt1	-0.63	0.027	0.317	-0.290	6.27E-03
Prrc2b	-0.47	0.045	0.349	-0.304	1.36E-02
Prrc2c	-0.58	0.080	0.413	-0.333	1.61E-02

Gene name	Average LogFc L *vs.* UL	pct L	pct UL	Δpct L-UL	Adjusted *P*-value
Psme2	-0.40	0.107	0.429	-0.322	5.00E-02
Ptprm	-0.59	0.027	0.317	-0.290	6.35E-03
R3hdm1	-0.94	0.018	0.365	-0.347	1.66E-05
Rab14	-0.45	0.098	0.413	-0.315	4.28E-02
Rapgef3	-0.56	0	0.190	-0.190	1.13E-02
Rasgrf2	-0.60	0.027	0.349	-0.322	6.47E-04
Rasip1	-0.42	0.152	0.524	-0.372	3.95E-03
Rbm25	-0.26	0.071	0.381	-0.310	9.35E-03
Rbm5	-0.58	0.027	0.302	-0.275	1.76E-02
Rbms1	-0.61	0.125	0.508	-0.383	2.37E-03
Rfc1	-0.26	0	0.190	-0.190	1.13E-02
Rhob	-0.42	0.196	0.587	-0.391	2.14E-03
Ripor1	-0.62	0.027	0.349	-0.322	5.35E-04
Rnf13	-0.61	0	0.254	-0.254	8.69E-05
Rpn2	-0.60	0.062	0.397	-0.335	4.67E-03
Rras	-0.65	0.143	0.556	-0.413	5.93E-04
Rsbn1l	-0.51	0.018	0.270	-0.252	2.91E-02
Rtn4	-0.74	0.062	0.429	-0.367	4.63E-04
Sar1b	-0.25	0.018	0.302	-0.284	6.69E-04
Scara3	-0.54	0	0.206	-0.206	3.40E-03
Scx	-0.48	0	0.175	-0.175	3.69E-02
Sdf4	-0.29	0.089	0.413	-0.324	1.68E-02
Sec14l1	-0.43	0.036	0.333	-0.297	6.36E-03
Sec31a	-0.47	0.054	0.349	-0.295	2.56E-02
Sfpq	-0.67	0.089	0.444	-0.355	5.92E-03
Sgms1	-0.50	0.018	0.270	-0.252	2.81E-02
Ski	-0.69	0.045	0.349	-0.304	1.20E-02
Slc38a2	-1.06	0.045	0.444	-0.399	1.34E-05
Smc1a	-0.50	0.054	0.349	-0.295	3.08E-02
Smim10l1	-0.52	0.089	0.429	-0.340	1.42E-02
Smpd1	-0.60	0	0.190	-0.190	1.13E-02
Sncg	-0.72	0.080	0.397	-0.317	4.28E-02
Sod3	-0.90	0.009	0.254	-0.245	1.01E-02
Spcs2	-0.68	0.098	0.476	-0.378	2.03E-03
Spock2	-0.92	0	0.175	-0.175	3.69E-02
Sptlc2	-0.34	0.036	0.333	-0.297	4.45E-03
Srek1	-0.60	0.027	0.302	-0.275	1.84E-02
Srsf11	-0.67	0.045	0.365	-0.320	4.44E-03
Srsf5	-0.61	0.161	0.556	-0.395	3.85E-03
Ssb	-0.50	0.098	0.444	-0.346	3.97E-03
Ssfa2	-0.97	0.036	0.333	-0.297	9.58E-03
Ssr3	-0.27	0.062	0.349	-0.287	4.17E-02
St3gal6	-0.43	0	0.175	-0.175	3.69E-02
Stk10	-0.42	0	0.222	-0.222	1.01E-03
Svil	-0.62	0.009	0.270	-0.261	2.40E-03

Gene name	Average LogFc L *vs.* UL	pct L	pct UL	Δpct L-UL	Adjusted *P*-value
Tacc1	-0.44	0.045	0.349	-0.304	7.22E-03
Taz	-0.29	0	0.175	-0.175	3.69E-02
Tcn2	-0.39	0.036	0.333	-0.297	9.39E-03
Tm9sf2	-0.44	0.027	0.317	-0.290	5.05E-03
Tm9sf3	-0.31	0.071	0.381	-0.310	2.29E-02
Tmed2	-0.72	0.107	0.508	-0.401	5.09E-04
Tmed5	-0.59	0.054	0.365	-0.311	1.42E-02
Tmem109	-0.34	0.045	0.333	-0.288	2.95E-02
Tmem176b	-0.95	0.107	0.619	-0.512	5.62E-08
Tmem184b	-0.55	0.027	0.317	-0.290	6.04E-03
Tmem88	-0.43	0.036	0.317	-0.281	2.50E-02
Tnfaip8	-0.92	0.045	0.333	-0.288	4.04E-02
Tppp3	-0.41	0.009	0.238	-0.229	1.59E-02
Tpr	-0.52	0.098	0.524	-0.426	1.92E-05
Tra2b	-0.65	0.062	0.381	-0.319	1.60E-02
Trim47	-0.87	0.054	0.476	-0.422	1.76E-06
Tubb4b	**-0.59**	**0.116**	**0.571**	**-0.455**	**2.40E-06**
Uaca	-0.64	0.071	0.381	-0.310	2.65E-02
Uqcr10	-0.40	0.196	0.556	-0.360	3.78E-02
Vcl	-0.78	0.018	0.286	-0.268	9.54E-03
Wdr61	-0.43	0	0.206	-0.206	3.40E-03
Wnk1	-0.39	0.107	0.444	-0.337	1.95E-02
Wwc2	-0.35	0.054	0.381	-0.327	3.03E-03
Xist	-1.32	0.018	0.286	-0.268	9.96E-03
Zbtb4	-0.71	0.027	0.349	-0.322	6.44E-04
Zbtb7a	-0.50	0.054	0.397	-0.343	4.72E-04
Zcchc11	-0.43	0.009	0.270	-0.261	2.93E-03
Zcchc6	-0.76	0.036	0.381	-0.345	3.37E-04
Zfhx3	-0.41	0	0.175	-0.175	3.69E-02
Zfp664	-0.50	0.036	0.317	-0.281	2.08E-02
Zfyve9	-0.41	0	0.175	-0.175	3.69E-02
Rpl17	0.79	0.973	0.841	0.132	9.27E-05
Rpl26	0.84	0.973	0.873	0.100	1.19E-06
Rpl28	0.90	0.964	0.825	0.139	4.84E-06
Rpl29	0.97	0.812	0.698	0.114	1.48E-04
Rplp2	0.90	0.938	0.794	0.144	3.27E-07
Rps10	0.95	0.929	0.825	0.104	1.04E-05
Rps19	0.95	0.964	0.857	0.107	1.95E-08
Rps24	0.87	1	0.889	0.111	2.26E-07
Rps28	0.86	0.946	0.825	0.121	1.75E-06

Genes related to prioritized functional terms (see Table VI and VII) are highlighted in **blue**. Genes are listed alphabetically. Downregulated genes are shaded in white, upregulated genes are shaded in gray. FAL: femoral artery ligation; Pct: percentage; L: ligated; UL: unligated. The obtained *P*-values were adjusted for multiple testing based on Bonferroni correction using all genes in the dataset.

Online Table V. Type B2 genes (*n*=181) uniquely altered by FAL in *EC-Prdm16*$^{-/-}$ mice

Gene Name	Average LogFc L *vs.* UL	pct L	pct UL	Δpct L-UL	Adjusted *P*-value
Abcb1a	-0.81	0.061	0.331	-0.270	2.89E-06
Ablim1	-0.66	0.193	0.462	-0.269	2.36E-02
Ablim3	-0.70	0.044	0.214	-0.170	1.74E-02
Acta2	-0.66	0.175	0.679	-0.504	6.86E-16
Afap1l2	-0.58	0.026	0.197	-0.171	1.78E-02
Afdn	-1.13	0.123	0.508	-0.385	2.37E-10
Ano6	-0.81	0.079	0.268	-0.189	2.10E-02
Apoe	**-1.57**	**0.167**	**0.656**	**-0.489**	**1.10E-16**
Aqp7	**-1.17**	**0.018**	**0.311**	**-0.293**	**8.31E-10**
Arhgef15	-0.67	0.114	0.355	-0.241	8.60E-03
Arhgef2	-0.76	0.088	0.318	-0.230	1.67E-03
Arl15	-0.55	0.035	0.201	-0.166	3.87E-02
Atp2a3	-0.73	0.079	0.301	-0.222	2.28E-02
Atxn7l3b	-0.42	0.140	0.401	-0.261	1.34E-02
B2m	-0.81	0.360	0.853	-0.493	3.99E-17
Bgn	-0.99	0.316	0.518	-0.202	4.58E-02
Bmp4	-1.12	0.132	0.331	-0.199	9.46E-03
Bpgm	-0.96	0.114	0.321	-0.207	2.41E-02
Btnl9	-1.39	0.026	0.308	-0.282	7.60E-09
C1qtnf9	-0.87	0.044	0.251	-0.207	6.69E-04
Cavin2	**-1.44**	**0.237**	**0.786**	**-0.549**	**3.32E-24**
Ccnl2	-0.57	0.061	0.281	-0.220	4.56E-03
Cd2ap	-0.74	0.140	0.492	-0.352	9.62E-07
Cd74	-1.55	0.088	0.258	-0.170	3.19E-02
Cd9	-0.97	0.237	0.552	-0.315	2.01E-04
Cdkn1a	-0.47	0.053	0.251	-0.198	2.29E-02
Clu	-0.81	0.184	0.468	-0.284	1.50E-03
Cmip	-0.79	0.053	0.284	-0.231	2.14E-04
Ckb	-0.65	0.026	0.231	-0.205	2.84E-03
Clec14a	-0.75	0.149	0.401	-0.252	1.32E-02
Cped1	-0.69	0.035	0.251	-0.216	2.45E-03
Cr1l	-0.60	0.088	0.344	-0.256	7.97E-04
Crip2	-0.80	0.368	0.769	-0.401	7.27E-10
Ctsd	-0.64	0.167	0.448	-0.281	4.08E-03
Ctsf	-0.29	0	0.127	-0.127	1.11E-02
Ctsh	-1.48	0.123	0.395	-0.272	7.63E-09
Ctsl	-0.57	0.193	0.525	-0.332	1.89E-05
Ddit4	-1.02	0.096	0.421	-0.325	2.04E-07
Ddx3x	-0.38	0.184	0.452	-0.268	1.32E-02
Dhh	**-0.54**	**0.018**	**0.191**	**-0.173**	**1.37E-02**
Dpm3	-0.70	0.114	0.418	-0.304	4.97E-05
Ebf1	-1.04	0.105	0.375	-0.270	4.67E-05
Ecscr	-0.28	0.316	0.575	-0.259	3.12E-02

Gene name	Av.rage LogFc L *vs.* UL	pct L	pct UL	Δpct L-UL	Adjusted *P*-value
Efnb1	-0.81	0.053	0.234	-0.181	3.04E-03
Ehd2	**-0.48**	**0.281**	**0.582**	**-0.301**	**3.72E-03**
Ephx1	-0.88	0.035	0.301	-0.266	2.33E-06
Etl4	-0.67	0.079	0.304	-0.225	5.63E-03
Fabp4	**-2.27**	**0.430**	**0.582**	**-0.152**	**3.68E-13**
Fabp5	**-1.71**	**0.105**	**0.388**	**-0.283**	**1.29E-04**
Fbln5	**-1.27**	**0.123**	**0.418**	**-0.295**	**3.55E-07**
Fmo1	-0.47	0.035	0.227	-0.192	2.07E-02
Fmo2	-0.66	0.061	0.294	-0.233	2.68E-03
Fn1	-1.33	0.140	0.401	-0.261	1.22E-03
Fgd5	-0.63	0.123	0.398	-0.275	1.51E-03
Fhl1	-0.74	0.026	0.258	-0.232	1.43E-04
Fus	-0.43	0.219	0.502	-0.283	8.68E-03
Gata2	-0.65	0.070	0.284	-0.214	1.05E-02
Gpihbp1	**-1.66**	**0.123**	**0.418**	**-0.295**	**3.16E-06**
Gstm1	-0.87	0.070	0.311	-0.241	4.96E-04
H2-T23	-0.82	0.070	0.321	-0.251	5.34E-06
Hnrnpu	-0.37	0.202	0.472	-0.270	1.44E-02
Hrct1	-0.61	0.044	0.258	-0.214	3.60E-03
Ifnar2	-0.65	0.079	0.291	-0.212	1.30E-02
Igfbp7	-1.04	0.263	0.522	-0.259	3.76E-02
Itm2b	-0.84	0.439	0.846	-0.407	6.22E-13
Jmjd1c	-0.72	0.044	0.254	-0.210	4.80E-03
Jup	-0.93	0.070	0.365	-0.295	1.43E-06
Kank3	-0.90	0.105	0.371	-0.266	5.63E-04
Kcnq1ot1	-0.79	0.053	0.237	-0.184	6.53E-03
Lamp1	-0.67	0.281	0.579	-0.298	3.82E-03
Limch1	-0.70	0.053	0.241	-0.188	2.86E-02
Lmo2	-0.85	0.254	0.492	-0.238	4.72E-02
Lmo7	-0.53	0.044	0.244	-0.200	1.08E-02
Lpar6	-0.72	0.123	0.381	-0.258	7.50E-03
Lpl	**-1.15**	**0.018**	**0.244**	**-0.226**	**1.37E-05**
Mcfd2	**-0.81**	**0.096**	**0.284**	**-0.188**	**8.24E-03**
Mef2a	-0.70	0.114	0.398	-0.284	1.62E-04
Mef2c	-0.86	0.114	0.421	-0.307	1.39E-05
Mettl7a1	-0.33	0	0.130	-0.130	7.67E-03
Mgp	**-1.67**	**0.412**	**0.736**	**-0.324**	**1.11E-06**
mt-Nd2	-0.32	0.886	0.993	-0.107	8.85E-05
mt-Nd4l	-0.80	0.237	0.635	-0.398	2.84E-08
mt-Nd5	-0.67	0.342	0.779	-0.437	1.51E-11
Myct1	-0.74	0.193	0.478	-0.285	1.37E-03
Myh11	-0.72	0.009	0.181	-0.172	3.15E-03
Myl6	**-0.40**	**0.711**	**0.910**	**-0.199**	**4.06E-02**
Myl9	**-0.80**	**0.044**	**0.274**	**-0.230**	**9.32E-04**

Gene name	Average LogFc L *vs.* UL	pct L	pct UL	Δpct L-UL	Adjusted *P*-value
Nfat5	-0.71	0.096	0.344	-0.248	3.91E-04
Nfib	-0.34	0.254	0.535	-0.281	6.07E-03
Nfic	-0.59	0.158	0.405	-0.247	4.88E-02
Pdia3	-0.86	0.158	0.475	-0.317	4.37E-05
Pdzd2	-0.77	0.035	0.234	-0.199	7.99E-04
Phf20l1	-0.56	0.088	0.318	-0.230	2.36E-02
Phlda3	**-0.86**	**0.114**	**0.304**	**-0.190**	**4.52E-02**
Pi16	-1.18	0.026	0.278	-0.252	9.49E-07
Pkp4	-0.62	0.096	0.338	-0.242	1.20E-02
Plec	-0.85	0.140	0.418	-0.278	1.06E-03
Prdx4	-0.85	0.140	0.361	-0.221	7.85E-03
Qk	-0.86	0.158	0.512	-0.354	6.15E-07
Ralbp1	-0.61	0.140	0.401	-0.261	1.38E-02
Rbp7	**-1.91**	**0.123**	**0.435**	**-0.312**	**3.44E-07**
Reep3	-0.78	0.149	0.478	-0.329	5.09E-06
Rgcc	-1.31	0.079	0.328	-0.249	9.49E-05
Rock2	-0.55	0.167	0.428	-0.261	1.25E-02
Rsad2	-0.92	0.044	0.224	-0.180	1.17E-02
S1pr1	-1.19	0.175	0.575	-0.400	6.96E-10
Selenom	-0.60	0.211	0.522	-0.311	5.89E-04
Selenop	-0.79	0.193	0.495	-0.302	5.09E-04
Sema3g	-1.05	0.053	0.291	-0.238	1.72E-05
Sgk1	-1.23	0.061	0.385	-0.324	6.32E-08
Shtn1	-0.39	0.018	0.187	-0.169	2.05E-02
Slfn5	-0.80	0.158	0.448	-0.290	6.37E-04
Sorbs2	-0.75	0.079	0.288	-0.209	1.63E-02
Spag9	-0.91	0.123	0.435	-0.312	7.00E-07
Sult1a1	-0.90	0.053	0.274	-0.221	7.10E-04
Syne1	-0.60	0.035	0.231	-0.196	2.22E-03
Syt7	-0.49	0	0.177	-0.177	3.74E-05
Tagln	-0.67	0.149	0.565	-0.416	3.42E-10
Tanc1	-0.88	0.079	0.301	-0.222	1.15E-03
Tap2	-0.65	0.088	0.308	-0.220	5.27E-03
Tbx3	-0.52	0.009	0.154	-0.145	3.87E-02
Tcf15	-0.93	0.061	0.288	-0.227	2.92E-03
Tcim	-0.90	0.096	0.308	-0.212	3.45E-02
Thrsp	-0.92	0	0.251	-0.251	5.43E-09
Timp4	**-1.62**	**0.009**	**0.308**	**-0.299**	**9.76E-11**
Tm6sf1	-0.74	0.096	0.321	-0.225	7.62E-03
Tmbim1	-0.64	0.053	0.328	-0.275	6.10E-06
Tmcc3	-0.70	0.061	0.291	-0.230	1.58E-03
Tmem140	-0.77	0.053	0.264	-0.211	2.46E-04
Tmem245	-0.78	0.070	0.288	-0.218	5.42E-04
Tpm1	-0.69	0.325	0.589	-0.264	3.14E-02

Gene name	Average LogFc L *vs.* UL	pct L	pct UL	Δpct L-UL	Adjusted *P*-value
Tpm2	-1.17	0.079	0.435	-0.356	1.88E-08
Trib2	-0.31	0	0.114	-0.114	4.90E-02
Ushbp1	-0.81	0.132	0.381	-0.249	1.19E-03
Vcam1	-1.09	0.096	0.304	-0.208	4.00E-03
Xdh	-0.70	0.009	0.207	-0.198	9.71E-05
Zcchc7	-0.71	0.096	0.294	-0.198	3.58E-02
Aprt	1.12	0.377	0.154	0.223	3.67E-05
Cotl1	0.67	0.149	0.007	0.142	6.21E-04
Eef1g	1.27	0.658	0.441	0.217	5.55E-20
Eef2	0.82	0.789	0.689	0.100	1.16E-12
Gapdh	1.05	0.754	0.609	0.145	2.72E-16
H2afz	1.19	0.535	0.398	0.137	4.01E-10
Hnrnpa1	1.07	0.553	0.361	0.192	3.43E-07
Marcksl1	0.93	0.246	0.007	0.239	1.51E-10
Mif	1.03	0.456	0.324	0.132	3.61E-05
Naca	0.69	0.825	0.702	0.123	9.06E-08
Npm1	1.40	0.816	0.485	0.331	5.00E-23
Pabpc1	1.00	0.588	0.438	0.150	1.37E-08
Pkm	0.96	0.526	0.391	0.135	1.31E-07
Ppp1r14b	1.03	0.439	0.237	0.202	8.81E-06
Ptpn18	0.96	0.298	0.107	0.191	2.76E-02
Rack1	0.99	0.912	0.753	0.159	3.93E-22
Ran	1.04	0.447	0.338	0.109	9.59E-06
Rbm3	1.08	0.596	0.401	0.195	7.94E-10
Rpl10	0.99	0.772	0.609	0.163	6.45E-14
Rpl10a	1.06	0.877	0.706	0.171	3.27E-20
Rpl11	0.79	0.886	0.756	0.130	1.20E-10
Rpl13a	0.81	0.465	0.311	0.154	2.76E-03
Rpl14	1.05	0.868	0.756	0.112	1.51E-24
Rpl22l1	0.92	0.684	0.555	0.129	4.16E-11
Rpl3	0.64	0.965	0.819	0.146	6.95E-10
Rpl36a	1.08	0.877	0.709	0.168	2.57E-24
Rpl4	1.06	0.728	0.569	0.159	2.09E-17
Rpl7a	0.98	0.816	0.645	0.171	1.74E-16
Rplp0	1.38	0.991	0.846	0.145	2.90E-47
Rps13	0.86	0.930	0.826	0.104	4.48E-16
Rps15a	1.01	0.974	0.870	0.104	3.12E-28
Rps17	0.92	0.851	0.709	0.142	2.38E-14
Rps2	1.49	0.991	0.836	0.155	1.05E-47
Rps6	1.19	0.939	0.736	0.203	3.10E-29
Rps9	0.93	1	0.863	0.137	6.74E-26
Rpsa	1.52	0.974	0.793	0.181	1.23E-52
S100a8	**1.10**	**0.140**	**0.007**	**0.133**	**2.77E-03**
S100a9	**1.21**	**0.228**	**0.007**	**0.221**	**3.09E-09**
Snn	1.07	0.316	0.064	0.252	4.36E-06

Gene name	Average LogFc L *vs.* UL	pct L	pct UL	Δpct L-UL	Adjusted *P*-value
Snrpe	0.75	0.526	0.425	0.101	4.72E-03
Snrpf	0.86	0.430	0.308	0.122	2.99E-04
Socs3	0.87	0.211	0.040	0.171	7.82E-03
Timp1	**1.08**	**0.211**	**0.017**	**0.194**	**4.26E-06**
Tubb6	0.78	0.211	0.033	0.178	3.65E-03

Genes related to prioritized functional terms (see Table VI and VII) are highlighted in **blue**. *Timp* genes are in **bold face**. Genes are listed alphabetically. Downregulated genes are shaded in white, upregulated genes are shaded in gray. FAL: femoral artery ligation; Pct: percentage; L: ligated; UL: unligated. The obtained *P*-values were adjusted for multiple testing based on Bonferroni correction using all genes in the dataset.

Online Table VI. KEGG Functional annotation analysis

	DAVID or GSEA Functional term	% of genes
Functional terms uniquely associated with type B1 genes		
1	KEGG_SPHINGOLIPID_METABOLISM	7.69
2	KEGG_VASOPRESSIN_REGULATED_WATER_REABSORPTION	6.82
3	KEGG_CARDIAC_MUSCLE_CONTRACTION	6.41
4	KEGG_NOTCH_SIGNALING_PATHWAY	6.38
5	KEGG_HUNTINGTONS_DISEASE	5.56
6	KEGG_OXIDATIVE_PHOSPHORYLATION	5.34
7	KEGG_ALZHEIMERS_DISEASE	4.85
8	KEGG_PARKINSONS_DISEASE	4.69
9	KEGG_TIGHT_JUNCTION	4.55
10	**KEGG_GAP_JUNCTION**	**4.44**
11	KEGG_LEUKOCYTE_TRANSENDOTHELIAL_MIGRATION	4.31
12	KEGG_REGULATION_OF_ACTIN_CYTOSKELETON	4.23
13	KEGG_FOCAL_ADHESION	4.02
14	mmu04141:Protein processing in endoplasmic reticulum	3.74
15	mmu04932:Non-alcoholic fatty liver disease (NAFLD)	2.80
16	**mmu04961:Endocrine and other factor-regulated calcium reabsorption**	**2.34**
17	KEGG_MAPK_SIGNALING_PATHWAY	2.25
Functional terms uniquely associated with type B2 genes		
1	**KEGG_PPAR_SIGNALING_PATHWAY**	**5.80**
2	KEGG_ANTIGEN_PROCESSING_AND_PRESENTATION	5.68
3	KEGG_AXON_GUIDANCE	4.65
4	KEGG_VASCULAR_SMOOTH_MUSCLE_CONTRACTION	4.35

Functional categories are sorted based on descending % of genes. Prioritized terms of interest are highlighted in **blue**. DAVID-related terms are in small caps, GSEA-related terms are in large caps. Numbers in the left column correspond to the X-axis value in Figure 6D.

Online Table VII. GO-MF Functional annotation analysis

	DAVID or GSEA Functional term	% of genes
Functional terms uniquely associated with type B1 genes		
1	GO:0005515~protein binding	32.71
2	GO_OLIGOSACCHARYL_TRANSFERASE_ACTIVITY	30.00
3	GO_CLATHRIN_LIGHT_CHAIN_BINDING	28.57
4	GO_G_PROTEIN_COUPLED_SEROTONIN_RECEPTOR_BINDING	28.57
5	GO_URIDYLYLTRANSFERASE_ACTIVITY	28.57
6	GO_JUN_KINASE_BINDING	22.22
7	**GO_LOW_DENSITY_LIPOPROTEIN_PARTICLE_RECEPTOR_BINDING**	**19.05**
8	GO:0000166~nucleotide binding	17.76
9	**GO_LIPOPROTEIN_PARTICLE_RECEPTOR_BINDING**	**15.38**
10	GO_NOTCH_BINDING	11.54
11	GO:0003676~nucleic acid binding	10.75
12	GO_PHOSPHATIDYLINOSITOL_3_4_5_TRISPHOSPHATE_BINDING	10.26
13	GO_ATP_DEPENDENT_MICROTUBULE_MOTOR_ACTIVITY_PLUS_END_DIRECTED	10.00
14	GO_MIRNA_BINDING	10.00
15	GO:0008270~zinc ion binding	9.35
16	GO_CLATHRIN_BINDING	7.02
17	GO_SMAD_BINDING	6.67
18	GO:0032403~protein complex binding	6.07
19	GO:0019901~protein kinase binding	6.07
20	GO_PDZ_DOMAIN_BINDING	5.81
21	GO_MOTOR_ACTIVITY	4.41
22	GO:0019904~protein domain specific binding	4.21
23	GO_ATPASE_ACTIVITY_COUPLED	3.50
24	GO_RHO_GTPASE_BINDING	3.43
25	GO_PHOSPHATIDYLINOSITOL_BINDING	2.86
26	GO:0005085~guanyl-nucleotide exchange factor activity	2.80
27	GO_ATPASE_ACTIVITY	2.51
28	GO_HYDROLASE_ACTIVITY_ACTING_ON_ACID_ANHYDRIDES	2.43
29	GO_GTPASE_BINDING	2.40
30	GO_TUBULIN_BINDING	2.35
31	GO_ENZYME_ACTIVATOR_ACTIVITY	2.12
32	GO_SMALL_GTPASE_BINDING	2.04
33	GO:0004579~dolichyl-diphosphooligosaccharide-protein glycotransferase activity	1.87
34	GO:0031072~heat shock protein binding	1.87
35	GO:0043014~alpha-tubulin binding	1.40
36	GO_RIBONUCLEOTIDE_BINDING	1.37
37	GO_ADENYL_NUCLEOTIDE_BINDING	1.23
38	GO_DRUG_BINDING	1.22
39	GO:0031826~type 2A serotonin receptor binding	0.93

	Functional terms uniquely associated with type B2 genes	
1	**GO_ARACHIDONIC_ACID_BINDING**	**40.00**
2	GO_N_N_DIMETHYLANILINE_MONOOXYGENASE_ACTIVITY	40.00
3	GO_ICOSANOID_BINDING	33.33
4	GO_ICOSATETRAENOIC_ACID_BINDING	33.33
5	GO_THYROID_HORMONE_BINDING	28.57
6	GO_5S_RRNA_BINDING	27.27
7	**GO_LONG_CHAIN_FATTY_ACID_BINDING**	**21.43**
8	GO_RAGE_RECEPTOR_BINDING	18.18
9	GO_TOLL_LIKE_RECEPTOR_BINDING	16.67
10	GO_STRUCTURAL_CONSTITUENT_OF_MUSCLE	16.28
11	GO_MYOSIN_HEAVY_CHAIN_BINDING	15.38
12	GO_RIBOSOMAL_LARGE_SUBUNIT_BINDING	15.38
13	GO:0005198~structural molecule activity	13.33
14	GO_POLY_PURINE_TRACT_BINDING	11.54
15	GO_RRNA_BINDING	11.29
16	**GO_FATTY_ACID_BINDING**	**11.11**
17	**GO_PROTEIN_LIPID_COMPLEX_BINDING**	**9.09**
18	GO_PROTEOGLYCAN_BINDING	8.33
19	GO_PEPTIDASE_ACTIVATOR_ACTIVITY	7.89
20	GO_KINASE_INHIBITOR_ACTIVITY	7.46
21	GO:0008092~cytoskeletal protein binding	7.27
22	GO_TAU_PROTEIN_BINDING	6.67
23	GO_NADH_DEHYDROGENASE_ACTIVITY	6.52
24	**GO_MONOCARBOXYLIC_ACID_BINDING**	**5.88**
25	GO_ACTIVATING_TRANSCRIPTION_FACTOR_BINDING	5.81
26	GO_NADP_BINDING	5.77
27	GO_RIBONUCLEOPROTEIN_COMPLEX_BINDING	5.38
28	GO_AMYLOID_BETA_BINDING	5.19
29	GO_STRUCTURAL_CONSTITUENT_OF_CYTOSKELETON	4.76
30	GO_SINGLE_STRANDED_RNA_BINDING	4.65
31	GO_KINASE_ACTIVATOR_ACTIVITY	4.60
32	GO_KINASE_REGULATOR_ACTIVITY	4.33
33	GO_PRIMARY_ACTIVE_TRANSMEMBRANE_TRANSPORTER_ACTIVITY	3.60
34	GO_TRANSLATION_REGULATOR_ACTIVITY	3.57
35	GO_PEPTIDASE_REGULATOR_ACTIVITY	3.15
36	GO:0005539~glycosaminoglycan binding	3.03
37	GO:0001871~pattern binding	3.03
38	GO:0030247~polysaccharide binding	3.03
39	GO_EXTRACELLULAR_MATRIX_STRUCTURAL_CONSTITUENT	3.03
40	GO_ENZYME_INHIBITOR_ACTIVITY	2.91
41	GO_RHO_GTPASE_BINDING	2.86
42	GO_HORMONE_RECEPTOR_BINDING	2.69
43	GO_PROTEIN_C_TERMINUS_BINDING	2.65

44	GO_DNA_BINDING_TRANSCRIPTION_FACTOR_BINDING	2.51
45	GO_RNA_POLYMERASE_II_SPECIFIC_DNA_BINDING_TRANSCRIPTION_FACTOR_BINDING	2.49
46	GO:0008201~heparin binding	2.42
47	GO_DNA_BINDING_TRANSCRIPTION_ACTIVATOR_ACTIVITY	2.34
48	GO_TRANSCRIPTION_FACTOR_BINDING	2.25
49	GO_ENZYME_ACTIVATOR_ACTIVITY	1.92
50	GO_CHROMATIN_BINDING	1.84
51	GO_CIS_REGULATORY_REGION_BINDING	1.79
52	GO_MRNA_BINDING	1.77
53	**GO_LIPID_BINDING**	**1.64**
54	GO_PROTEIN_HOMODIMERIZATION_ACTIVITY	1.64
55	**GO_CALCIUM_ION_BINDING**	**1.57**
56	GO_PROTEIN_DIMERIZATION_ACTIVITY	1.52
57	GO_OXIDOREDUCTASE_ACTIVITY	1.47
58	GO_REGULATORY_REGION_NUCLEIC_ACID_BINDING	1.35
59	GO_SEQUENCE_SPECIFIC_DOUBLE_STRANDED_DNA_BINDING	1.35
60	GO_RIBONUCLEOTIDE_BINDING	1.00

Functional categories are sorted based on descending % of genes. Prioritized terms of interest are highlighted in **blue**. DAVID-related terms are in small caps, GSEA-related terms are in large caps. Numbers in the left column correspond to the X-axis value in Figure 6D.

1

Online Table VIII. List of genes associated with prioritized functional terms

A. Type B1 genes associated with selected functional terms

Functional term(s)	*Gene name/symbol*	*General information*	*Involved in (endothelial) cell (dys)function?*			
			Ca2+ homeostasis?	*eNOS/NO?*	*Redox status?*	*Caveolae/clathrin?*
• **Endocrine and other factor-regulated Ca^{2+} reabsorption** • **Lipoprotein particle receptor binding** • **Clathrin binding***	***Ap2a1*** Adaptor Related Protein Complex 2 Subunit Alpha 1	- encodes α1 adaptin subunit of the adaptor protein 2 (AP-2) complex found in **clathrin**-coated vesicles. The AP-2 complex links **clathrin** to receptors in vesicles - interacts with **DnaJa1** - Only ENU mice available, no phenotypic analysis has been reported - has been associated with cardiovascular disease and blood pressure in GWAS studies (Gene Cards website)	-the AP2 complex is involved in **Ca^{2+} homeostasis** through internalization of the calcium-sensing receptor, which in turn leads to impaired **Gnaq/11** signaling			- regulates **clathrin**-coated vesicle size and maturation
• **Endocrine and other factor-regulated Ca^{2+} reabsorption**	***Atp1a1*** ATPase Na^+/K^+ Transporting Subunit Alpha 1	- encoded protein belongs to the family of Na^+/K^+-ATPases; Na^+/K^+-ATPase is an integral membrane protein responsible for establishing and maintaining the electrochemical gradients of Na^+ and K^+ across the plasma membrane - the other subunit (Atp1a2) of the Na^+/K^+-ATPase has been shown to be among the most downregulated genes during mesenteric collateral growth in rats	- implicated in **Ca^{2+} homeostasis** through interaction with the Na^+/Ca^{2+} exchanger - heterozygous deficiency for the Na^+/K^+-ATPase subunits causes abnormalities in cardiac contraction in part through **Ca^{2+} homeostasis regulation**			- has been associated with (caveolin-1 in) **caveolae** in ECs
• **Endocrine and other factor-regulated Ca^{2+} reabsorption** • **LDLr binding** • **Clathrin binding*** • **Clathrin light chain binding***	***Cltc*** Clathrin Heavy Chain	- **clathrin** heavy chain is a major protein component of the cytoplasmic face of intracellular organelles, called coated vesicles and pits; these organelles are involved in the intracellular trafficking of receptors and endocytosis of a variety of macromolecules -The basic subunit of the **clathrin** coat is composed of 3 heavy and 3 light chains. - No KO mice currently reported - is likely involved in hepatocytic **endocytosis of LDL receptor**	- **clathrin**-coated vesicles play a role in **Ca^{2+} homeostasis** through intracellular trafficking of Ca^{2+}-specific receptors, including TRPV5			- **clathrin** heavy chain is a major protein component of the cytoplasmic face of intracellular endocytotic organelles, called coated vesicles and coated pits
• **LDLr binding**	***Dnaja1*** DnaJ Heat Shock Protein Family (Hsp40) Member A1	- encodes a member of the DnaJ family of proteins, which act as heat shock protein 70 co-chaperones. Heat shock proteins facilitate protein folding, trafficking, prevention of aggregation, and proteolytic degradation. - Plays a role in protein transport into mitochondria via its role as co-chaperone.				

		- Promotes apoptosis in response to cellular stress - *DnaJa1*-deficient mice have a compromised antibody immune response - DnaJa1-deficiency causes abnormal spermiogenesis and aberrant androgen receptor signaling - was cloned from a HUVEC cDNA library				
• **Gap junction** • **Endocrine and other factor-regulated Ca^{2+} reabsorption**	***Gnaq*** G Protein Subunit Alpha Q ***Gna11*** G Protein Subunit Alpha 11	- encode guanine nucleotide-binding proteins which couple a seven-transmembrane domain receptor to activation of PLCβ - are part of a **gap junction** network - endothelial Gnaq is, together with Gna11, involved in VEGF-induced vascular permeability and angiogenesis - *Gnaq* KO causes impaired motor coordination and platelet aggregation	- Gnaq is involved in **Ca^{2+} homeostasis** through PLCβ-mediated conversion of PIP_2 to IP_3 and through relieving Ca^{2+}/Na^+ channel TRPV4 inhibition - are involved in **Ca^{2+} handling** in cardiomyocytes - Gnaq is involved in **Ca^{2+} handling** in platelets	- are involved in regulation of eNOS activation through regulation of **Ca^{2+} transients**		- found to be localized in lipid rafts together with **caveolins** in lung microvascular ECs
• **Lipoprotein particle receptor binding** • **Clathrin binding*** • **Clathrin light chain binding***	***Hip1r*** Huntingtin Interacting Protein 1 Related	- Gene Ontology (GO) annotations related to this gene include *actin binding* and ***phosphatidylinositol binding***. - **Component of clathrin-coated pits and vesicles**, that may link the endocytic machinery to the actin cytoskeleton. - Binds 3-phosphoinositides (via ENTH domain). May act through the ENTH domain to promote cell survival by stabilizing receptor tyrosine kinases following ligand-induced endocytosis. **- its paralog Hip1 binds to AP2; Hip1r itself does not directly bind AP2 and has a lower affinity for clathrin** - mice deficient in HiP1r are viable and normal but have accelerated spinal abnormalities and dwarfism when also being deficient for HIP, hence HIP can compensate for the loss of Hip1r - little HIP1r staining in peripheral nerves and blood vessel endothelium				- **Component of clathrin-coated pits and vesicles**, that may link the endocytic machinery to the actin cytoskeleton. - mouse embryonic fibroblasts (MEFs) showed no abnormalities in constitutive or stimulated clathrin-mediated endocytosis in the *Hip1r* knockout background.
• **Gap junction**	***Pdgfb*** Platelet Derived Growth Factor Subunit B	- encodes a member of the protein family comprised of both platelet-derived growth factors (Pdgfs) and vascular endothelial growth factors (Vegfs). Pdgf-b is a growth factor for mesenchymal cells and has a particularly important role in the recruitment of pericytes during angiogenesis				

		- its receptor Pdgfrb is part of a **gap junction** network - has been shown to disrupt **gap junction** communication in mesangial cells through phosphorylation of Cx43 - pericytes fail to be recruited to developing blood vessels in mice null for *Pdgfb* or *Pdgfrb*, thereby leading to vascular dysfunction and perinatal death - EC-specific loss of *Pdgfb* causes loss of pericytes in the retinal vasculature				
• **Lipoprotein particle receptor binding** • **LDLr binding** • **Clathrin binding***	***Picalm*** Phosphatidylinositol Binding Clathrin Assembly Protein (Synonym: *Calm*)	- encodes a clathrin assembly protein, which recruits clathrin and adaptor protein complex 2 (AP2) to cell membranes at sites of coated-pit formation and clathrin-vesicle assembly. - **binds membrane phospholipids and *1-phosphatidylinositol*** - modulates autophagy and the turnover of autophagy substrates - in the brain, Picalm is predominantly present in ECs - *Calm*-deficient mice have severe anemia and Calm is required for erythroid maturation and transferrin internalization - is expressed in kidney ECs - Interacts with **AP2A1**		- increased expression levels of Calm in ECs of the corpus cavernosum have been associated with increased (phosphorylated) **eNOS levels**		**- regulates clathrin-coated vesicle size and maturation**
• **Gap junction**	***Tubb4b*** Tubulin Beta 4B Class IVb (synonym: *Tubb2c*, *Tubb2*)	- encodes the β2 subunit of tubulins which is a major constituent of microtubules - KO not commercially available, has cardiovascular phenotype (Gene Cards website) - is part of a **gap junction** network - intact microtubules are involved in membrane targeting of Cx43 and formation of **gap junctions**				- microtubules play a role in stabilization and recycling of **caveolae** and trafficking towards myoendothelial junctions - glycosylation of β2 (and β3) tubulin regulates **caveolae**-mediated internalization of Tgfβ receptors in human microvascular ECs during EndoMT - silencing of Tubb4b opposes the EndoMT-elicited decrease in **caveolae** in human microvascular ECs

B. Type B2 genes associated with selected functional terms

Functional term(s)	*Gene name/symbol*	*General information*	*Involved in (endothelial) cell (dys)function?*			
			Ca2+ homeostasis?	*eNOS/NO?*	*Redox status?*	*Caveolae/clathrin?*
• **Lipid binding** **LDLr binding**	***Apoe*** Apolipoprotein E	- encodes a major apoprotein of the chylomicron and is essential for the normal catabolism of triglyceride-rich lipoprotein constituents. - mediates **lipoprotein clearance** through the uptake of chylomicrons, VLDLs, and HDLs by hepatocytes - by participating in the lipoprotein-mediated distribution of lipids among tissues, APOE plays a critical role in plasma and tissue **lipid homeostasis** - APOE is also involved in reverse cholesterol transport - in blood vessels, expression has been documented in SMCs		- ubiquitous ApoE deficiency results in **EC dysfunction** caused by reduced endothelial NO synthase enzyme activity - while exogenous ApoE has been shown to differentially increase eNOS production in an isoform-specific manner in ECs through expression of the apoER2 in these cells, the role of endogenous apoE remains unknown - ubiquitous ApoE knock-out mice have **impaired endothelium-dependent relaxation** in femoral arteries upon induction of temporal ischemia in the hind limb	- ubiquitous ApoE deficiency results in **endothelial dysfunction** caused by increased **production of O_2^-**	
• **Ppar signaling pathway**	***Aqp7*** Aquaporin 7	- encodes a member of the aquaporin family of water-selective membrane channels. The encoded protein localizes to the plasma membrane and allows movement of water, glycerol and urea across cell membranes. - highly expressed in the adipose tissue where the encoded protein facilitates efflux of glycerol[56] - is present in spermatids, as well as in the testicular and epididymal spermatozoa - plays an important role in body energy homeostasis under conditions that promote lipid catabolism, giving rise to glycerol and free fatty acids. - expressed in capillary ECs from adipose tissue, cardiac and striated muscle - a **downstream target of Ppar-gamma** in adipose tissue and in heart ECs				

		- Mice deficient in *Aqp7* have lower plasma glycerol levels, loss of glycerol in urine, become obese and develop insulin resistance				
• **Lipid binding**	***Cavin2*** Caveolae Associated Protein 2 (synonym: SDPR: serum deprivation-response protein)	- encodes an adaptor protein present in caveolae and is a calcium-independent **phospholipid-binding** protein whose expression increases in serum-starved cells. - is required for *in vitro* EC proliferation, migration and invasion - is highly expressed in different EC types		- regulates the **production of NO** in ECs by controlling its stability and activity in a caveolae-independent manner; Cavin-2 knockdown ECs produce less NO		- Regulates **caveolae morphology** by inducing membrane curvature - Plays a role in **caveolae formation** in a tissue-specific manner. (required in lung and fat but not in heart endothelia) - mice lacking cavin-2 have perturbed lung EC morphology, barrier function and show loss of caveolae in lung and adipose tissue ECs
• **Ca^{2+} binding**	***Dhh*** Desert Hedgehog Signaling Molecule	- encodes a member of the hedgehog family. containing signaling molecules that play an important role in regulating morphogenesis. - Dhh is mainly expressed in the peripheral nerves and male gonads but also in ECs of large vessels -In adults, the Hh pathway has been shown to be reactivated after ischemic injury, including hind limb ischemia - hedgehog family members promote angiogenesis through non-canonical signaling pathways - absence of Dhh causes **endothelial dysfunction** (*i.e.*, increase permeability) in endoneural capillaries, which has been linked to neuropathy[68] - Dhh knockdown in ECs promotes endothelial permeability and EC activation and a Dhh agonist prevents TNF-α or glucose-induced EC dysfunction and significantly improved EC function **without promoting angiogenesis**	- **Ca^{2+} binding** modulates its interaction with surface receptors	- a Dhh agonist restores **impairment in EC-dependent relaxation**		
• **Ca^{2+} binding**	***Ehd2*** EH Domain Containing 2	- encodes a member of the EH domain-containing protein family and plays a role in membrane trafficking between the plasma membrane and endosomes - is expressed in ECs of arteries -in adipocytes and fibroblasts, loss of *Ehd2* leads to increased fatty acid uptake	- by controlling caveolar dynamics, EHD2 orchestrates **Ca^{2+} channel localization** at the plasma membrane; Following an ATP stimulus, reduced	- impaired relaxation of mesenteric arteries were observed in *Ehd2* knockout mice. *Ehd2* deletion or knockdown led to decreased production		- interacts with the actin cytoskeleton and binds to an EH domain-binding protein. This interaction appears to connect **clathrin-**

			cytosolic Ca^{2+} peaks were recorded in HUVECs lacking EHD2	of NO although eNOS expression levels were not changed. eNOS was less phosphorylated at Ser1177 and was redistributed from the plasma membrane to internalized detached caveolae in EHD2-lacking tissue or cells		**dependent endocytosis** to actin - *Ehd2* loss in small arteries led to increased numbers of **caveolae** that were detached from the plasma membrane. - Regulates the equilibrium between cell surface-associated and -dissociated **caveolae** by constraining caveolae at the cell membrane
• **Lipid binding** • **(Long chain) FA binding** • **Monocarboxylic acid binding** • **Ppar signaling pathway**	***Fabp4*** Fatty Acid Binding Protein 4 ***Fabp5*** Fatty Acid Binding Protein 5	- encode the fatty acid binding proteins mainly found in adipocytes (Fabp4) or found in multiple cell types (Fabp5), including epidermal cells, adipocytes, macrophages, and alveolar epithelial cells . Fatty acid binding proteins are a family of small, highly conserved, cytoplasmic proteins that **bind long-chain fatty acids** and other hydrophobic ligands. - FABPs have a role in fatty acid uptake, transport, and metabolism. - Fabp4 and Fabp5 are co-expressed in a subset of mostly microvascular and small vessel ECs, while Fabp5 is also detected in ECs of larger blood vessels (including the aorta) - Fabp4 is a mediator of VEGF/hypoxia-induced angiogenesis *in vitro* and *in vivo* - FABP5-deficient ECs are significantly more resistant to apoptotic cell death and FABP5 deficiency leads to a profound impairment in EC proliferation and chemotactic migration		- exogenous FABP4 inhibits **eNOS production**, activation and NO production[84] - elevated expression of intracellular FABP4 in human microvascular ECs contributes to their dysfunction through a reduction of **eNOS phosphorylation** - exposure to VEGF of FABP4-deficient ECs leads to attenuation of angiogenic responses, such as cell proliferation, migration, survival, and morphogenesis, in part through **downmodulation of eNOS signaling**		
• **Ca^{2+} binding**	***Fbln5*** Fibulin 5	- encodes a secreted, extracellular matrix protein - expressed predominantly in the VSMCs of developing arteries in mouse embryos; lower levels of expression are also observed in ECs; mRNA expression is dramatically downregulated in adult arteries - it colocalizes with the endothelium in atherosclerotic vessels	- fibulin 5 is a **Ca^{2+}-binding** protein through its EGF-like domains		- **regulates vascular redox state** by binding extracellular superoxide dismutase (thus preserving NO activity); superoxide anion production was	

		- defects in this gene are a cause of autosomal dominant cutis laxa, autosomal recessive cutis laxa type I (CL type I), and age-related macular degeneration type 3 (ARMD3) - is essential for elastogenesis *in vivo* - has a context-dependent effect on angiogenesis sometimes functioning as an inhibitor or a supporter - ubiquitous KO mice have decreased arterial inner diameter and compliance and abnormal diastolic function[98] - ubiquitous KO mice have altered vascular remodeling through a role in SMC proliferation and migration			increased in *Fbln5*$^{-/-}$ aortas	
• **Lipid binding** • **LDLr binding** • **Ppar signaling pathway****	***Gpihbp1*** Glycosylphosphatidylinositol Anchored High Density Lipoprotein Binding Protein 1	- encodes a capillary EC protein that facilitates the lipolytic processing of triglyceride-rich lipoproteins by **transporting lipoprotein lipase** (LPL) from the subendothelial spaces to the capillary lumen (and back) - Anchors LPL on the surface of ECs in the lumen of blood capillaries - is **induced by Pparγ**				- transcellular transport of Gpihbp1-LPL complexes occurs through vesicular transport, but is independent of **caveolin-1**
• **Ca^{2+} binding** • **Lipid binding** • **Ppar signaling pathway** • **LDLr binding**	***Lpl*** Lipoprotein Lipase	- encodes lipoprotein lipase, which is expressed in heart, muscle, and adipose tissue. LPL has the dual functions of triglyceride hydrolase and ligand/bridging factor for **receptor-mediated lipoprotein uptake** - catalyzes the hydrolysis of triglycerides from circulating chylomicrons and very low density lipoproteins (VLDL), and thereby plays an important role in **lipid clearance** from the blood stream, lipid utilization and storage - recruited to its site of action on the luminal surface of vascular endothelium by binding to GPIHBP1 and cell surface heparan sulfate proteoglycans - is expressed in organ parenchymal cells, but was recently also shown to be expressed by endothelial cells in the heart	- **Ca^{2+}** is important for LPL homodimerization and activation	- mice overexpressing human Lpl in ECs have upon Tnfα exposure impaired **endothelium-dependent relaxation**, caused by a **reduction in eNOS dimers** -mice overexpressing human LpL in VSMCs have impaired **endothelium-dependent relaxation**		- found to be localized in lipid rafts together with **caveolins** in lung microvascular ECs
• **Ca^{2+} binding**	***Mcfd2*** Multiple Coagulation Factor Deficiency 2, ER Cargo Receptor Complex	- encodes a soluble luminal protein with two **calmodulin-like EF-hand motifs** - currently no info about a role in ECs - *Mcfd2*-deficient mice are viable and demonstrate reduced plasma FV, FVIII and α1-antitrypsin levels	- forms a **Ca^{2+}-dependent** complex with lectin mannose binding protein 1 that functions as a cargo receptor and facilitates			

		- RNA expression has been detected human LSECs and HUVECs	the transport of FV and FVIII from the ER to the Golgi apparatus			
• **Ca^{2+} binding**	***Mgp*** Matrix Gla Protein	- encodes a member of the osteocalcin/matrix Gla family of proteins - is expressed in vascular tissue by both SMCs and endothelium - mice lacking *Mgp* show spontaneous arterial calcification - *Mgp*-deficient ECs adopt characteristics of mesenchymal stem cells and may be prone to EndoMT - mice lacking *Mgp* have arteriovenous malformations by affecting BMP-Notch cross-talk - there is a correlation between arterial calcification and ischemia in PAD	- is a 10-kDa polypeptide containing **Ca^{2+}-binding** carboxyglutamic acid (Gla) residues and three phosphoserines			
• **Ca^{2+} binding**	***Myl6*** Myosin Light Chain 6 ***Myl9*** Myosin Light Chain 9	- encode myosin light chains that are expressed in smooth muscle and non-muscle tissues; they regulate muscle contraction by modulating the ATPase activity of myosin heads - No KO reported - currently nothing about a role in ECs for Myl6 - Myl9 expression in rat iliac arteries is increased in endothelium upon aging and after injury - Myl9 causes contraction, paracellular gap formation and hyperpermeability of ECs - knockdown of *Myl9* in ECs causes impaired migration	-The encoded proteins **bind Ca^{2+}** and are activated by myosin light chain kinase.			
• **Lipid binding**	***Phlda3*** Pleckstrin Homology Like Domain Family A Member 3	- Phlda3 binds phosphatidylinositol second messengers (***phosphatidylinositol-4,5-bisphosphate binding* and *phosphatidylinositol-3-phosphate*).** - expressed in trophoblasts - is transiently expressed in the DA during zebrafish development - mice lacking Phlda3 expression are viable but have placental overgrowth - phlda3 overexpression impairs hemangioblast specification and vascular (ISV) development in zebrafish - Phlda3 overexpression attenuates and cardiomyocyte-specific KO aggravates cardiac hypertrophy after banding or AngII exposure		- does not affect eNOS activation downstream of p53		

• **Lipid binding** • **Ppar signaling pathway****	***Rbp7*** Retinol Binding Protein 7	- encodes a member of the cellular **retinol-binding protein** (CRBP) family, whose members are required for vitamin A stability and metabolism. - Is a member of the Fabp family - is a **PPARγ target gene** enriched in (or even restricted to) vascular ECs - expression of RBP7 is mostly restricted to ECs from small vessels			- is required to **mediate the anti-oxidative effects of PPARγ** in the endothelium through adiponectin - RBP7-deficient mice exhibit normal EC function at baseline but exhibit severe endothelial dys-function through oxidative stress (**incl. increased Nox expression**) in response to cardiovascular stressors	
• **Ca^{2+} binding** • **Lipid binding** • **Fatty acid binding** • **Long chain fatty acid binding** • **Monocarboxylic acid binding** • **Arachidonic acid binding**	***S100a8*** S100 Calcium Binding Protein A8 ***S100a9*** S100 Calcium Binding Protein A9	- proteins encoded by these genes are members of the S100 proteins are released from monocytes, SMCs and ECs in response to stress - Ca^{2+}- and Zn^{2+}-binding proteins which play a prominent role in inflammatory processes and immune response - preferentially exists as a heterodimer or heterotetramer known as calprotectin which has a wide plethora of intra- and extracellular functions. The intracellular functions include: facilitating **arachidonic acid trafficking** - S100a8/a9 can promote atherosclerosis - low concentrations of exogenous S100a8/9 promote angiogenic activity of ECs - calprotectin facilitates **fatty acid uptake** through CD36 in ECs as part of a complex with **arachidonic acid** - a null mutation in *S100a8* is embryonic lethal; *S100a9* KO is viable	- S100 family members of proteins contain 2 **Ca^{2+}-binding** motifs - calprotectin increases permeability of EC monolayers in a **Ca^{2+}-dependent** way - calprotectin is involved in **regulating Ca^{2+} influx** in monocytes in response to VEGF165b - **Ca^{2+} signaling** in *S100a9* null neutrophils downstream of PLC is impaired		- the extracellular functions of calprotectin involve proinflammatory, **oxidant-scavenging** and apoptosis-inducing activities.	
• **Lipid binding**	***S1pr1*** Sphingosine-1-Phosphate Receptor 1 (synonym: *S1p1)*	- encodes a receptor for **sphingolipid** S1P - structurally similar to G protein-coupled receptors and is highly expressed in ECs - Inhibits sprouting angiogenesis to prevent excessive sprouting during blood vessel development - mice lacking S1p1r die *in utero* - EC-specific deletion results in defective vascular maturation		- HDL contains **S1P and in this way induces eNOS activation and NO production and vasodilation** through S1P3 rather than S1P1 -both $S1P_1$ and $S1P_3$ activation result in **NO production via Akt-**		- S1P1 co-localizes with caveolin-1 in **caveolae** and this association inhibits downstream NO production - S1P1 along with PAR-2 mediates EC-dependent vasorelaxation in aortas and this functional interaction is

		- S1P1 responds to S1P as well as laminar shear stress to transduce flow-mediated signaling in ECs both *in vitro* and *in vivo*		**mediated eNOS stimulation** in HUVECs		dependent of their co-localization in **caveolae**
• **Ca^{2+} binding** • **Lipid binding**	***Syt7*** Synaptotagmin 7	- encodes a member of the synaptotagmin family similar to other family members that mediate **Ca^{2+}-dependent** regulation of membrane trafficking in synaptic transmission - Involved in **cholesterol transport** from lysosome to peroxisome by promoting membrane contacts between lysosomes and peroxisomes - involved in exocytosis of secretory and synaptic vesicles through **Ca^{2+} and phospholipid binding** - KO available, is viable and currently no vascular phenotype reported - *Syt* KO mice display a lower body weight, reduced body fat content, a higher basal metabolic rate, and an increased rate of lipolysis compared with wild-type mice - expressed in HUVECs and co-localizes with WPB and lysosomes (J. Frampton, PhD thesis) - its family member Syt5 is involved in Weibel-Palade body exocytosis in human ECs	- **Ca^{2+} sensor** involved in **Ca^{2+}-dependent** exocytosis of secretory and synaptic vesicles - SYT7 is required for synaptic vesicle replenishment by acting as a sensor for Ca^{2+} and by forming a complex with calmodulin			

Information in columns relevant to the corresponding functional terms is highlighted in **blue**. Genes that encode proteins that are closely related family members are grouped together. Cases where proteins encoded by different genes from the list interact with each other are highlighted in **green**. Involvement with caveolae is indicated in **red.** *Note that functional terms related to clathrin are highlighted in **purple** as they were not among the selected terms. However, several genes associated with the selected functional terms are also related to clathrin (heavy chain) binding. **Note that Ppar signaling pathway is highlighted in **orange** as this gene was not part of the KEGG pathway list despite its documented role as Ppar signaling target.